Universidade de Aveiro Secção Autónoma das Ciências da Saúde
2014

Cláudia Sofia Nunes Busca

Análise do Papel das Proteínas ZP3 e APP na Adesão Célula-Célula

Analysis of the Role of ZP3 and APP Proteins in Cell-Cell Adhesion

Universidade de Aveiro Secção Autónoma das Ciências da Saúde
2014

Cláudia Sofia Nunes Busca

Análise do Papel das Proteínas ZP3 e APP na Adesão Célula-Célula

Analysis of the Role of ZP3 and APP in Cell-Cell Adhesion

Dissertação apresentada à Universidade de Aveiro para cumprimento dos requisitos necessários à obtenção do grau de Mestre em Biomedicina Molecular, realizada sob a orientação científica da Professora Doutora Sandra Vieira, Professora auxiliar convidada da Secção Autónoma das Ciências da Saúde da Universidade de Aveiro.

Este

Programa Operacional Factores de Competitividade – COMPETE e por F –
para a Ciência e a Tecnologia no âmbito dos projetos PTDC/BEX-BCM/0493/2012, e PEst-OE/SAU/UI0482/2011.

Este trabalho é dedicado à minha família e amigos aos quais devo mais do que algum dia poderei retribuir. Adoro-vos.

o júri

presidente

Prof. Doutora Ana Gabriela Cavaleiro Henriques
Professora Auxiliar Convidada da Secção Autónoma das Ciências da Saúde da Universidade de Aveiro

Prof. Doutora Ana Sofia Direito dos Santos Duarte
Professora Auxiliar Convidada da Universidade de Aveiro

Prof. Doutora Sandra Isabel Moreira Pinto Vieira
Professora Auxiliar Convidada da Secção Autónoma das Ciências da Saúde da Universidade de Aveiro

agradecimentos

À minha orientadora, Professora Doutora Sandra Vieira, um agradecimento especial pelo apoio e dedicação incansável durante a realização de todo este trabalho. Obrigada pela motivação e generosidade. Muito obrigada por tudo!

À Professora Doutora Odete da Cruz e Silva pela oportunidade de participar neste projeto.

Ao pessoal do Centro de Biologia Celular, o meu muito obrigada por tudo aos colegas do laboratório de neurociências pela cooperação e boa disposição. Obrigada Regina, Ana Marote, Roberto e Joana Rocha pela vossa paciência e ajuda.

À Sandra, Cátia, Margarida, Sílvia, Dani e Rita, obrigada pelo vosso companheirismo e por partilharem comigo momentos de descontração e por estarem lá mesmo nos momentos de maior tensão.

À Soraia, nem tenho palavras para te agradecer. Muito obrigada de coração!

Ao Tiago, pelo apoio, paciência e carinho. Sem ti acredita não teria coragem de chegar até aqui!

palavras-chave

Adesão Celular; Proteina Percursora de Amilóide de Alzheimer (APP); Glicoproteina 3 da Zona Pelúcida (ZP3); Interação Proteína-Proteína e Célula-Célula

resumo

Entre os diversos tipos de interações entre células que ocorrem no organismo, a interação entre o oócito e o espermatozoide é de grande importância para a perpetuação da espécie. A adesão celular é então um processo fundamental para a fertilização, a qual envolve a zona pelúcida (ZP) dos oócitos, a primeira barreira encontrada pelos espermatozoides que medeia a primeira interação entre os gâmetas. A ZP3 é uma das principais proteínas da ZP, e ainda não se conhece qual o seu ligando no espermatozoide. A glicoproteína APP foi descrita por nós como estando presente na cabeça do espermatozoide, em particular na zona equatorial, envolvida na interação espermatozoide-oócito. Esta proteína é central à patogénese da Doença de Alzheimer e os seus papéis fisiológicos ainda não estão bem caracterizados. Este trabalho focou-se na caracterização de um possível interação entre a APP e a ZP3 na adesão célula-célula. Foi realizado um levantamento de motivos funcionais relevantes no ZP3, e avaliado o papel deste e da APP na adesão célula-célula. Para tal foram realizados ensaios de interferência com anticorpos contra epitopos da APP, da ZP3, e também da β1-integrina, um proteína importante na adesão celular e que se sabe ligar à APP. A co-localização subcelular entre a ZP3 e a APP foi analisada por imunocitoquímica, e uma possível interação física entre a ZP3 e APP monitorizada através de ensaios de imunoprecipitação. Os resultados indicam que, de entre as proteínas estudadas, a APP e a β1-integrina são as mais importantes na adesão celular, provavelmente através de uma via comum. A ZP3 parece ter apenas um pequeno efeito na adesão célula-célula, possivelmente através da mesma via da APP e da β1-integrina. Surpreendentemente, ZP3 e APP apresentam pouca co-localização, e especialmente em vesiculas perto do complexo de Golgi. Contudo, existe um maior grau de co-localização entre a ZP3 e a β1-integrina, particularmente perto da membrana plasmática. Inesperada foi também a presença de agregados extracelulares de ZP3 secretada contendo também APP. Os resultados preliminares dos ensaios de imunoprecipitação sugerem uma interacção física entre as formas altamente glicosiladas da APP e da ZP3, o que pode refletir uma importante interação destas duas proteínas na ZP do oócito aquando da fertilização.

keywords

Cellular Adhesion; Alzheimer's Amyloid Precursor Protein (APP); Zona Pellucida Glycoprotein 3 (ZP3); Protein-Protein and Cell-Cell Interaction

abstract

Among different types of cell-cell interactions present in the body, the interaction between the oocyte and a sperm cell is of great importance for species perpetuation. Cellular adhesion is thus a crucial process in fertilization, which involves the oocyte's zona pellucida (ZP), the first barrier found by sperm cells that mediates the first contact between gametes. ZP3 is a major ZP glycoprotein of the oocyte, and its ligand in sperm cells is still unknown. The APP glycoprotein was found by us to be in the sperm's head, including its equatorial zone involved in sperm-oocyte interaction. This protein plays a role in the pathogenesis of the Alzheimer's disease and its physiologic roles are still being unravelled. The present work aimed to characterize a putative APP-ZP3 interaction in cell-cell adhesion. Relevant functional motifs on the ZP3 amino acid sequence were analysed, and the role of ZP3 and APP in cell-cell adhesion was evaluated. Interference assays were performed with antibodies against epitopes of APP, ZP3 and β1-integrin, the latter an important protein in cellular adhesion known to bind APP. The subcellular co-localization of ZP3 and APP was analysed by immunocytochemistry assays, and a potential physical interaction between ZP3 and APP was evaluated by immunoprecipitation. Results indicate that, from the studied proteins, APP and β1-integrin are the most important in cell-cell adhesion, probably through a common pathway. ZP3 has only a minor effect in cell-cell adhesion, but is able to interfere with adhesion mediated by APP and β1-integrin, potentially sharing their common pathway. Surprisingly, ZP3 and APP only co-localize at low quantities in vesicles, mainly near the Golgi apparatus, while there is a slightly higher degree of co-localization between ZP3 and β1-integrin near the plasma membrane. Unexpectedly though, ZP3 and APP were found to co-localize in extracellular aggregates of secreted ZP3. Immunoprecipitation results so far further suggest that highly glycosylated ZP3 and APP forms physically interact, what may reflect an important interaction between these proteins in the oocyte's ZP upon fertilization.

Index

1. Abbreviations..... 3
2. Introduction..... 5
2.1. Zona Pellucida (ZP) Glycoproteins 6
2.1.1. Evolution of ZP Genes..... 7
2.1.2. Structure and Function of ZP Glycoproteins..... 10
2.1.2.1. Zona Pellucida Glycoprotein 1 (ZP1)..... 10
2.1.2.2. Zona Pellucida Glycoprotein 2 (ZP2) 11
2.1.2.3. Zona Pellucida Glycoprotein 3 (ZP3)..... 11
2.1.2.4. Zona Pellucida Glycoprotein 4 (ZP4)..... 12
2.1.3. Secretion and Assembly of ZP Glycoproteins..... 13
2.1.4. Proteins in Sperm-Egg Interactions..... 16
2.1.5. Sperm Proteins Involved in Sperm-Egg Interactions……..... 17
2.1.5.1. GalT..... 17
2.1.5.2. A Desintegrin and A Metalloproteinase (ADAM)..... 17
2.1.5.3. Zonadhesin..... 18
2.1.5.4. IZUMO..... 19
2.1.6. Oocyte Proteins Involved in Sperm-Egg Interactions..... 19
2.1.6.1. Integrins..... 19
2.1.6.2. CD9..... 20
2.2. Alzheimer's Amyloid Precursor Protein (APP)……..... 21
2.2.1. APP Proteolytic Processing..... 22
2.2.2. APP Isoforms..... 23
2.2.3. APP Dimerization..... 26
2.2.4 APP in Sperm Cells..... 27
3. Aims of the Thesis..... 29
4. Materials and Methods..... 31
4.1.ELM Bioinformatic Tool..... 31
4.2. Cell Culture..... 31
4.2.1. Cell Lines and Maintenance Conditions..... 31
4.2.1.1 HeLa Cells..... 31

4.2.1.2. CHO Cells.....32
4.2.1.3. HeLa-CHO co-cultures 32
4.3. Antibodies.....32
4.4. Cellular Adhesion Assays.....33
4.4.1. Optimization of CHO-HeLa Adhesion Assays.....33
4.4.2. Antibody Interference Assays.....34
4.5. Immunocytochemistry (ICC) Assays.....34
4.6. Immunoprecipitation.....35
4.7. Western Blot Assays.....36
5. Results.....39
5.1. *In Silico* Characterization of ZP3 Functional Motifs.....39
5.1.1. ZP3 Cleavage Sites.....39
5.1.2. ZP3 Binding Motifs.....41
5.1.3. ZP3 Ligand Motifs.....43
5.1.4. ZP3 Modifications.....44
5.1.5. ZP3 Trafficking.....48
5.2. Cell-cell adhesion assays.....49
5.2.1. Procedure optimization.....49
5.2.2 Characterization of CHO and HeLa Cells Adhesion.....53
5.2.3 Antibody Interference Assays.....56
5.3. Immunocytochemistry Assays.....60
5.4. Immunoprecipitation Assays.....64
6. Discussion and Conclusions.....67
7. References.....73
Appendix.....81

1. Abbreviations

aa	Amino acids
Aβ	Abeta peptide
AD	Alzheimer's Disease
ADAM	A Desintegrin And Metalloproteinase
AICD	APP Intracellular Cytoplasmic Domain
APLPs	APP-like Proteins
APP	Alzheimer's Amyloid Precursor Protein
CCA	Cell-Cell Adhesion
CFCS	Consensus Furin Cleavage Site
CHO	Chinese Hamster Ovary
CK1	Casein Kinase 1
CK2	Casein Kinase 2
CSF	Cerebrospinal Fluid
CuBD	Copper-Binding Domain
DB	Dynabeads
DMEM	Dulbelco's Minimum Essential Media
DSP	Dithiobis(succinimidyl propionate)
ECM	Extracellular Matrix
EHP	External Hydrophobic Path
ELM	Eukaryotic Linear Motif
FBS	Foetal Bovine Serum
GSK3	Glycogen Synthase Kinase 3
HGly	Heavily Glycosylated
HMW	Heavy Molecular Weight

ICC	Immunocytochemestry
IHP	Internal Hydrophobic Patch
IP	Immunoprecipitation
KPI	Kunitz Protease Inhibitor
LB	Loading Buffer
MAPK	Mitogen Activated Protein Kinase
MB	Millipore Beads
NDR	N-arginine Dibasic Convertase
ODf	Final Optic Density
PKA	Protein Kinase A
PKC	Protein Kinase C
PC6B	Proprotein Convertase 6B
PC7	Proprotein Convertase 7
PI3K	Phosphatidyl-Inositol-3-Kinase
PM	Plasma Membrane
ROI	Region Of Interest
RT	Room Temperature
WB	Western Blot
ZP	Zona Pellucida
ZP-C	Zona Pellucida Domain C-Terminus
ZP-N	Zona Pellucida Domain N-Terminus
ZP1	Zona Pellucida Glycoprotein 1
ZP2	Zona Pellucida Glycoprotein 2
ZP3	Zona Pellucida Glycoprotein 3
ZP4	Zona Pellucida Glycoprotein 4

2. Introduction

Among the various cell-cell interactions that can occur in the body, the interaction between the sperm and oocyte germ cells is one of crucial importance in species perpetuation. Molecular adhesion can be permanent or transitory, maintaining cells in contact with each other or enabling cell signalling, respectively. The adhesion events involved in fertilization are mainly transitory. Only the final event, the fusion of both gametes culminating in the formation of a zygote, is permanent. Adhesion is a critical event for appropriate oocyte selection within the ovary and its transport to the Fallopian Tubes, and to sperm-oocyte binding and gamete fusion. Altering adhesion properties can lead to ectopic pregnancies or infertility [1].

Oocyte activation by sperm is divided into three stages: oocyte-sperm recognition and binding; oocyte-sperm fusion; and polyspermy blockage. Following ejaculation, the sperm cell will encounter the oocyte when in the female Fallopian Tubes, and the recognition between these two cells involves the oocyte's zona pellucida (ZP). ZP is an acellular fibrous and noncollagenous glycoproteinaceous matrix that surrounds all mammalian oocytes (Figure 1) [2]–[5] [6]. The name is derived from Latin and means transparent belt or girdle. ZP is a porous layer, permeable to some macromolecules, such as antibodies [4], [7]. The ability to penetrate through is not only dependent on size, but also on the chemical and physical characteristic of the molecules [4]. ZP is assembled during the late stages of oogenesis when oocytes start to grow, increasing in thickness with oocyte development. Their relationship is so close that several studies report that production of ZP is crucial for oocyte growth and follicular development [7]. ZP is also involved in the binding of sperm during fertilization, being an important species-specific barrier, which results in oocyte penetration and leads to gametes fusion [5], [8], [9].

The binding of sperm to the ZP triggers the acrosome reaction of the bound sperm cell through the activation of several signal transduction cascades in the sperm. The acrosome reaction culminates in the fusion of the acrosome outer membrane with the sperm's plasma membrane, resulting in the exocytosis of the acrosome's contents: protease zymogenes, ZP ligands and other ligand-binding

proteins [10]. These enzymes allow the sperm cells to penetrate the ZP and the periviteline space, and the sperm must remain bound to the oocyte in order for this process to occur. Following this, the sperm and oocyte plasma membranes will fuse. The initial contact occurs between the tip of the sperm cell head and the oocyte plasma membrane, and then the side of the sperm cell head attaches to the oocyte. The fusion is thought to involve the central region of the sperm's head, near the equatorial region [1]. After the fusion occurs, several signalling pathways are activated, including an increase in the oocyte intracellular calcium levels. These lead to the completion of the oocyte meiosis and to the exocytosis of cortical granules from the oocyte, which contain enzymes that alter the ZP matrix and block polyspermy [5], [8], [9].

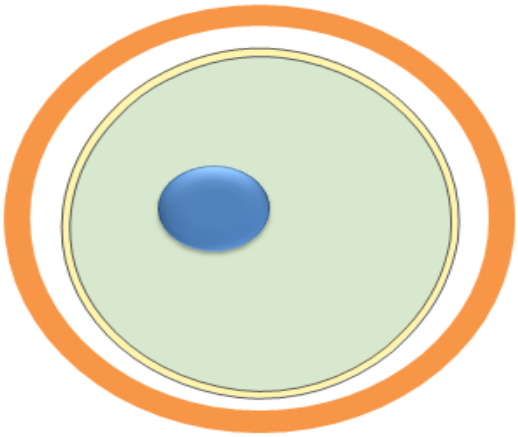

Figure 1. Schematic image of an oocyte with the nucleus (in blue), perivitelline space (white) surrounded by the zona pellucida (orange).

2.1. Zona Pellucida (ZP) Glycoproteins

Human ZP is composed by four glycoproteins: ZP1, ZP2, ZP3 and ZP4 [2]. Each consists of a polypeptide chain that is heterogeneously glycosylated with mannose and N-acetylglucosamine in the core of N-linked oligosaccharides and serine/threonine O-linked oligosaccharides [4]. Human ZP has a unique carbohydrate composition very different from other mammalian species [11]. Glycosylation has been demonstrated to be crucial for inducing acrosome

reaction, especially N-linked glycosylation. However, contrary to previous publications, it was found not indispensable for sperm binding [12]. Besides its role in sperm-egg interactions, glycosylation is also important for maintaining hydration in the matrix [13]. Polylactosamine, fucose and sialic acid residues are also present in human ZP. Analysis of the carbohydrate composition of ZP also revealed that the more compact area of ZP is closer to the oocyte, and the more porous area is in contact with follicular cells, being involved in sperm-oocyte interactions. In terms of composition, the porous region accounts for approximately 25% of the external area of the ZP, whereas the compact constitutes the remaining 75% [11].

All ZP proteins share a similar structure: a N-terminal hydrophobic signal sequence to direct them into a secretory pathway, a ZP domain of approximately 260 amino acids, a consensus furin cleavage site (CFCS) upstream of a transmembrane domain (TMD), which is followed by a short cytoplasmic tail [3], [14]. The ZP domain includes 8 conserved cysteine residues and a high β-strand content with conservation of polarity and hydrophobicity and turn tendency, which precedes the hydrophobic TMD. The ZP domain is present in several other extracellular proteins and is involved on protein-protein interactions [15].

2.1.1. Evolution of ZP Genes

ZP genes coding for ZP glycoproteins have been divided into six subfamilies: *zpa/zp2*, *zpb/zp4*, *zpc/zp3*, *zp1*, *zpax* and *zpd*. Phylogenetic analysis suggested that the first event in evolution was a gene duplication, originating *zpc*'s ancestral gene and the precursor of the other subfamilies. In the *zpb* subfamily a gene duplication appears to be responsible for two paralogous genes: *zp1* and *zp4*, implying that they had a common ancestral gene. *zpb/zp4* is a pseudogene in mouse which is a gene that evolved by insertions or deletions that resulted in premature stop codons, changing the reading frame and compromising the ability to code for a protein. The *zpb/zp4* pseudogene in the mouse was originated by a microdeletion of 19 nucleotides leading to a frameshift. Similarly, in bovine, *zp1* is also a pseudogene, resulting from microinsertions and a stop codon in chromosome 29. In humans, *zpax* is a pseudogene located on chromosome

2p24.2, resultant of a stop codon in exon 5. Lastly, *zpd* pseudogenes were reported absent from the mammalian genome. The identification of pseudogenes implied that evolution of *zp* genes occurs by death of genes.

The presence of *zp1* in chickens points to a duplication of its ancestral before the divergence between birds and mammals. The absence of *zpax* in primates suggests that loss of the gene occurred before the divergence between humans and other primates. In mammals, only primates and rodents have *zp1*, indicating that the loss of the gene occurred after the divergence between those groups and other mammals.

The presence of both *zpa/zp2* and *zpc/zp3* in all the analysed species implies a functional importance for the proteins they code for. Overall, this suggests that the interaction between sperm and oocyte involves ZPA/ZP2 plus ZPC/ZP3, and either ZPB/ZP4 or ZP1, or both [14].

Other studies suggest that *zp2* and *zp3* are rapid evolving genes under Darwinian positive selection, emphasising two evolutionary models: the sexual conflict model, in which optimal strategies concerning reproduction are conflicting between males and females, and the sperm competition model that highlights the competition between sperm cells of two different males to fertilize one female [16]. The positive selection exerted on them is thought to arise by the selective pressure from sperm-egg interactions [17].

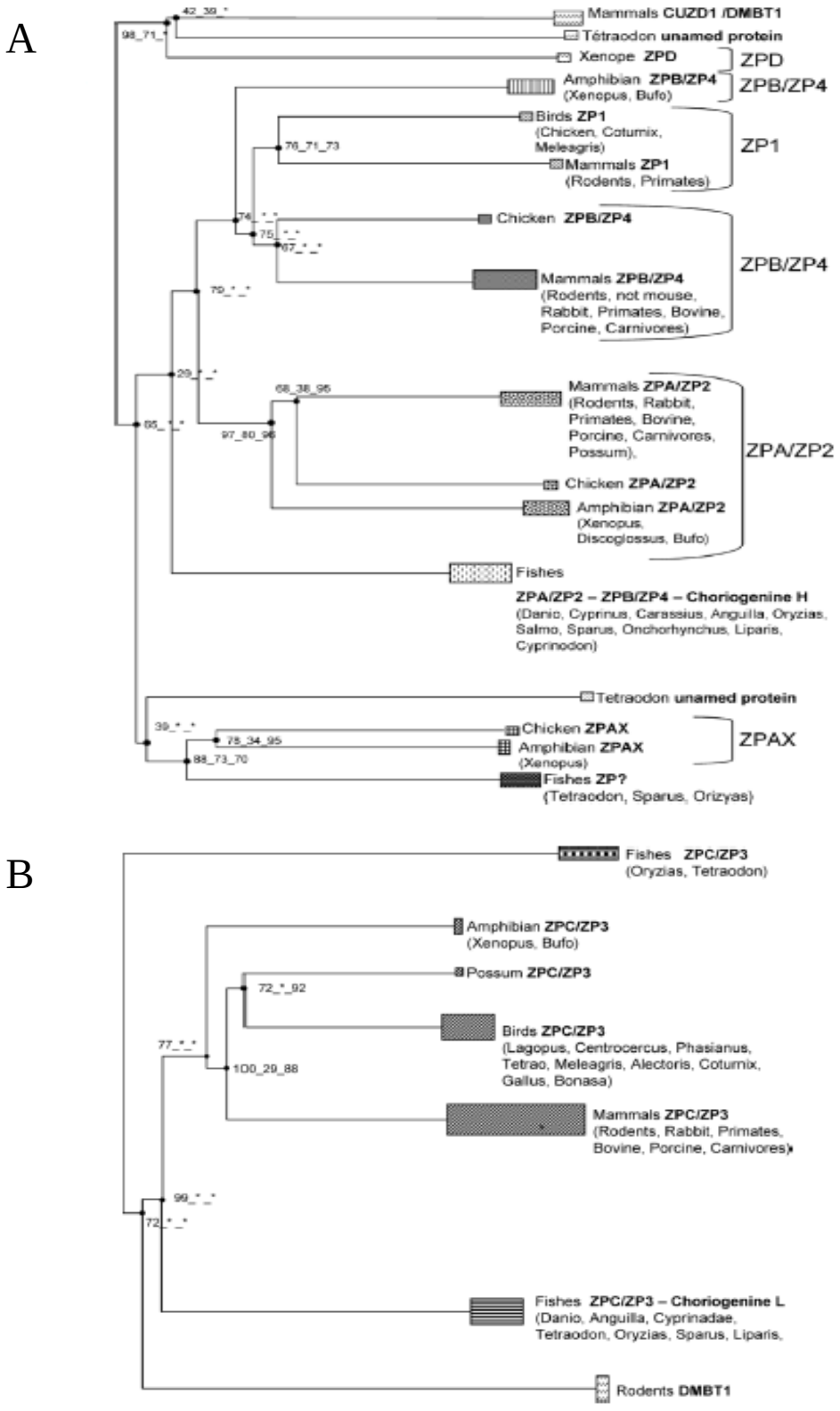

Figure 2. A. Phylogenetic tree of *zp1, zp2, zp4, zpax* and *zpd*, **B.** Phylogenetic tree of *zp3*. Genes used for comparisons are shown. The trees were obtained by FIGENIX BLAT of porcine ZPA/ZP and ZPC/ZP3 sequences, respectively. Branch length represents rates of evolution and values at tree nodes are bootstrap values. Retrieved from Goudet, G. et al (2008) [13].

2.1.2. Structure and Function of ZP Glycoproteins

ZP glycoproteins belong to a family of proteins called “zona pellucida domain proteins”, a heterogeneous family characterized by the presence of a ZP domain in their sequence [18]. This domain is a bipartide structure, with an N-terminus (ZP-N) and a C-terminus (ZP-C) and two conserved duplicated motifs, an internal hydrophobic patch (IHP) between the ZP-N and the ZP-C, and an external hydrophobic patch (EHP) further downstream the ZP-C (Figure 3 below) [19], [20]. These glycoproteins are known to be produced during the early stages of development, but their source is still debatable, having several studies suggested that in humans they are synthesized by both the oocyte and follicular cells [4], [9], [21]. Taking into account that the oocyte has a low capacity for protein synthesis, a role for follicular cells in the production of ZP proteins arose. Moreover, *in vitro* studies have shown that follicular cells are able to produce ZP components [4].The synthesis of each protein appears to occur independently despite their coordinated gene transcription [13]. Furthermore, synthesis of zona pellucida is thought to be associated with their heterogeneous distribution in the matrix and that may be associated with sperm penetration [11].

Each ZP glycoprotein has its singularities with different amino acid and oligosaccharide compositions, precursors, immunological reactivities and biological functions [9]. Indeed, despite having amino acid sequences highly conserved between vertebrates, their glycosylation patterns are species-specific [22].

2.1.2.1. Zona Pellucida Glycoprotein 1 (ZP1)

Human ZP1 is a 90-100 kDa glycoprotein composed by 638 amino acids [23], [24]. ZP1 has a trefoil domain with six conserved cysteines linked by disulfide bonds, upstream of the ZP domain, also present in ZP4 [13]. Early studies in mice identified six potential N-linked glycosylation sites in ZP1 [25]. A few studies indicated that ZP1 had only a structural function, mediating no interactions between oocytes and sperm cells [22]. However, some more recent reports suggest that during fertilization ZP1 binds to capacitated sperm cells and its glycosylation pattern is important for inducing acrosome reaction [3]. This

induction is independent of G_i protein-coupled receptor pathways and involves T-type and L-type voltage-operated calcium channels (VOCCs) [24].

2.1.2.2. Zona Pellucida Glycoprotein 2 (ZP2)

The human ZP2 is composed of 745 amino acids, and in prophase I the full length glycoprotein has 105-110 kDa [22], [24]. N-linked glycosylation comprises approximately 37% of its mass whereas O-linked glycans reflect only 8% [22]. ZP2 was implicated in polyspermy blockage. After egg-sperm fusion cortical granules are released by the oocyte, where a ZP2-specific protease cleaves the glycoprotein in the amino terminal domain, originating a protein with 60-73 kDa. A recent study in mice revealed that ZP2 is cleaved by ovastacin, an oocyte-specific metalloendoprotease. Indeed, ovastacin was found in cortical granules prior to fertilization, but not after. Furthermore, female mice lacking this protease fail to cleave ZP2 [26]. The cleavage of ZP2 induces hardening of the oocyte's zona pellucida, and changes in the mechanical properties of the matrix resultant from filament compaction, preventing binding of another spermatozoon [19], [23]. Furthermore, several studies demonstrate that ZP2 acts as a secondary sperm receptor through the biding of its N-terminal to acrosome-reacted spermatozoa, facilitating the penetration of the oocyte [27]. Hence, sperm cells cannot bind to the cleaved ZP2, blocking polyspermy [23]. Another role that has been attributed to ZP2 involves its cooperation with ZP3 in triggering acrosome reaction. The first appears to induces the release of Ca^{2+}, facilitating the induction of acrosome exocytose mediated by the latter [22].

2.1.2.3. Zona Pellucida Glycoprotein 3 (ZP3)

ZP3 is by far the most studied of all the ZP proteins. The human *zp3* gene has approximately 18,3 kbp and contains 8 exons, ranging from 92-312 kbp [28]. ZP3 has an N-terminal hydrophobic signal sequence of 22 amino acids, the ZP domain, and a tetrabasic CFCS sequence (^{349}RNRR^{352}) upstream of its TMD located at the 387-409 amino acids (Figure 3). The mature protein has 12 cysteine residues, 8 of each conserved between species, forming four disulfide bonds. The ZP domain ranges from the 45 to the 304 residues, its N-terminus is followed by

an IHP with 167-173 amino acids and its C-terminus is followed by an EHP with 362-368 amino acids [29].

Human *zp3* codes for a glycoprotein with 57-73 kDa and 424 amino acids [22], [24]. 27% of ZP3 molecular weight are N-linked oligosaccharides and only 9% O-linked glycans [22]. Early studies suggested that there was also a truncated form of this protein with only 372 amino acids, but this was never confirmed [21]. Recombinant ZP3 was shown to trigger acrosome reaction, being suggested as a primary sperm receptor [23].

The role of ZP3 glycosylation remains controversial but has been reported as crucial for inducing acrosome reaction, although the polypeptide chain is responsible for the binding to spermatozoa [29]–[31]. In humans, acrosome reaction mediated by ZP3 is dependent only on N-linked glycans, contrary to what occurs in mice, where it is mediated by O-linked oligosaccharides. Recurring to inhibitors, it was shown that acrosome reaction is induced by PKC (protein kinase C), T-type Ca^{2+}, extracellular Ca^{2+} and G-protein signalling [30]. Native ZP3 binds to the midpiece of intact spermatozoa, being the binding site lost after the induction of acrosome reaction [22]. The binding of sperm to ZP3 has also been correlated with its stimulatory action on sperm hyperactivation, implying that the sperm cells that bind ZP3 (and undergo acrosome reaction) are the motile ones [22], [32]. It was also hypothesized that due to the ZP3 unique disulfide linkage pattern in the ZP domain, different from other ZPs, the ZP C-terminus is responsible for the induction of the acrosome reaction [29]. A study by Baibakov and co-workers has provided evidence that binding of sperm to ZP is not sufficient for inducing the acrosome reaction, stating the importance of a mechanosensory signal produced during the oocyte penetration [22], [33].

2.1.2.4. Zona Pellucida Glycoprotein 4 (ZP4)

ZP4 is a 540 amino acids glycoprotein with a molecular weight of approximately 65 kDa [22]. This glycoprotein appears to have only N-linked glycosylation comprehending 18% of its molecular mass [22], [24]. A few studies have demonstrated that human ZP4 is also capable of inducing acrosome reaction, having a biding site in the acrosomal region of sperm cells [22], [30], [31].

Similarly to ZP3, acrosome reaction is also triggered exclusively by N-linked oligosaccharides and mediated by PKC, T-type Ca^{2+} channels and extracellular Ca^{2+}. Contrary to ZP3, it is independent of G-protein signalling but relies on PKA (protein kinase A) and L-type Ca^{2+} channels [30].

Crystallography studies shown that there are two types of ZP domain: a first found in ZP3, and a second one found in the other ZPs. Its two subdomains, ZP-N and ZP-C are separated by a protease-sensitive region [19], [34], [35].

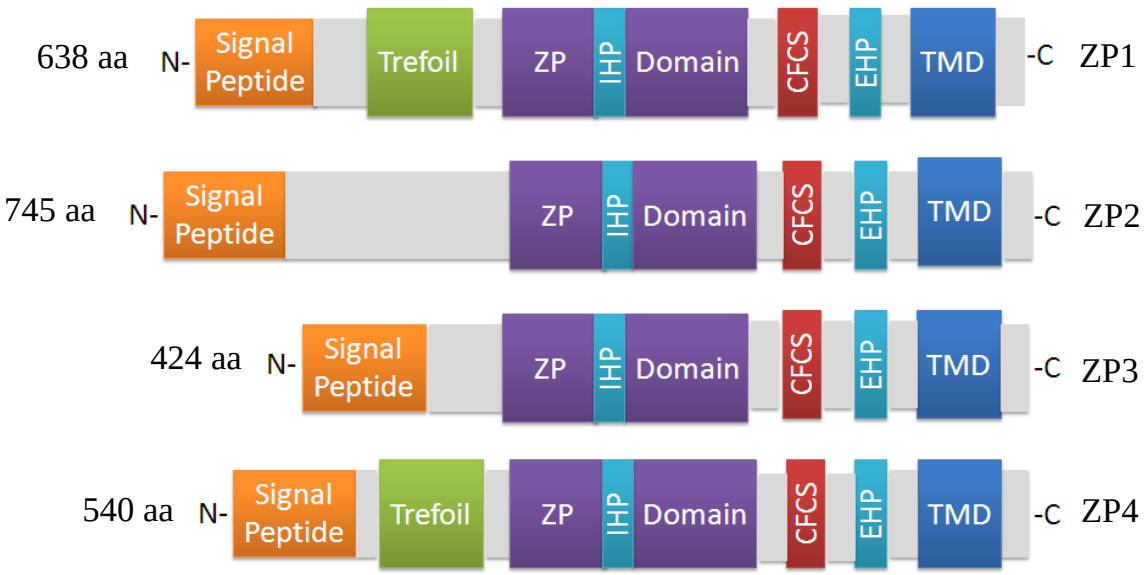

Figure 3. Schematic representation of ZPs. aa, amino acids; IHP, internal hydrophobic patch; CFCS, consensus furin cleavage site; TMD, transmembrane domain; EHP, external hydrophobic patch.

2.1.3. Secretion and Assembly of ZP Glycoproteins

The processes of synthesis, secretion and assembly of ZP proteins occur simultaneously [35]. Using a mouse model it was possible to study the secretion and assembly of these glycoproteins, with their secretion being reported not to be uniform [3]. The N-terminal signal peptide directs the precursor to a secretory pathway, first starting at the endoplasmic reticulum (ER) where the N-terminal

(signal peptide) is cleaved and the protein is folded and modified with high mannose type, N-linked oligosaccharides [35]. Then, the protein transits to the Golgi apparatus where its O-linked oligosaccharides are added [3], [35], [36]. During secretion, but before incorporation into the matrix, the precursor is cleaved extracellularly at the plasma membrane by furin-like convertases in its CFCS [20], [35]–[37]. The specific enzyme has not been described, but it is thought to be furin, PC6B (proprotein convertase 6B) or PC7 (proprotein convertase 7), since they all have transmembrane domains upstream of their C-termini, just like ZPs, and co-localize with these in the secretory pathway, facilitating ZPs cleavage [37]. This cleavage process was also validated for human ZP proteins [37].

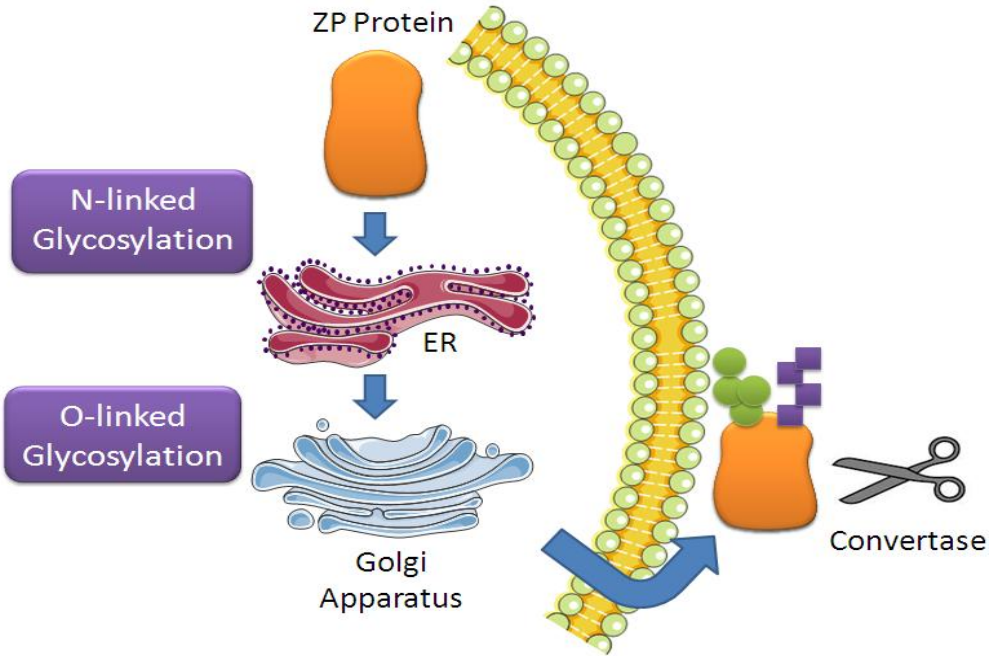

Figure 4. ZP glycosylation pathway and cleavage. Green circles represent N-linked glycans and purple squares are O-linked glycans.

When oocytes begin to grow, extracellular ZP glycoproteins are organized into filaments forming a hexagonal array with a uniform pore (Figure 5). The ZP domain is considered essential for their assembly into filaments, being actually present in several other proteins that are incorporated into matrices [38]. It is also present on uromodulin, α and β-tectorin and in the transforming growth factor-β receptor III (TGF-βR3) [39].

Upon cleavage within the CFCS there is dissociation of the mature secreted peptide and the C-terminus containing the short external hydrophobic patch (EHP), between the CFCS and the TMD, which seems crucial for protein secretion [19], [20]. *S*eparation between the secreted peptide and the EHP is associated with protein activation, inducing polymerization through the ZP domain [19], [20]. The IHP also mediates assembly, but appears to have no role in protein secretion. Lastly, the TMD is considered essential for propeptide cleavage and assembly, although indirectly, and does not seem to be involved in protein secretion [35], [38].

In mice, activation of ZP2 and ZP3 leads to their association into dimers that are bound to ZP1 homodimers by dissulfide bounds, forming filaments [9], [35]. Hence, ZP filaments are glycoprotein complexes of interspersed homo and hetero dimmers [30]. Incorporation of ZP3 into the ZP was also shown to depend on the presence of IHP [20]. A few years ago, some studies also showed the presence of ZP3-ZP2 dimers, crosslinked with ZP1 and ZP4 in humans [17], [18].

When the oocyte increases in size, these pores fuse originating a uniform matrix. Concomitantly, there is an increase in the number of microvilli that come in contact with follicular cells, establishing communication between them and the oocyte. It is thought that ZPs traffic through the oocyte without oligomerization, preventing premature assembly [3], [19], [40]. Indeed, ZP2 and ZP3 appear to traffic independently inside their secreting cell, and interactions between them are only seen after their incorporation into the ZP extracellular matrix [3], [19], [40]. ZP2 and ZP3 cytoplasmic tails appear to prevent interactions between them due to the hydrophilic nature of their basic amino acid residues [36], [40]. ZPs incorporation is believed to occur in the innermost surface of the ZP matrix, suggesting that ZP thickens from the inside [3]. ZP can reach a thickness of 13-16 µm in a mature human oocyte [4]. The mechanism of assembly of the ZP matrix is conserved from fish to mammals, suggesting that the conclusions reported from mice egg coat studies could be extrapolated to the human ZP [20].

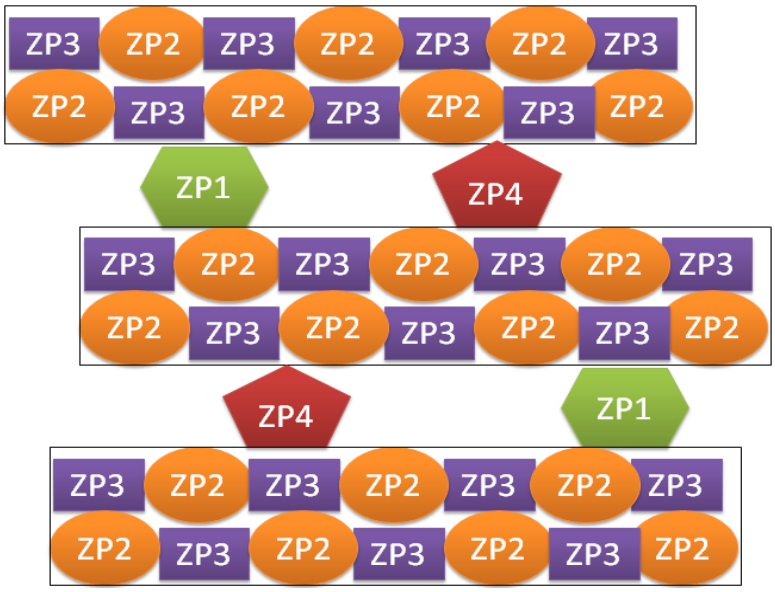

Figure 5. Schematic representation of human ZP filaments. ZP filaments are constituted by ZP2 and ZP3 (orange and purple, respectively), interconnected by monomers of ZP1 and ZP4 (green and red, respectively).

2.1.4. Proteins in Sperm-Egg Interactions

The interactions between sperm cells and oocytes are still unclear, and several models have been proposed: some argue that the gametes interact by carbohydrate moieties, others trough protein-protein interactions and finally protein-carbohydrate interactions have also been discussed [24]. Of all the mentioned above, the most accepted is the latter [3], [12], [29]–[31].

For more than 15 years, the prevailing model for sperm-egg binding was based on adhesion between an integrin on the oocyte and its ligand on the spermatozoon [1]. Integrins are membrane receptor proteins composed of two subunits, α and β, and are involved in cellular adhesion [17]. After several studies using knockout mice for the α_6 integrin subunit, this showed no significant reduction in sperm binding, and their role in sperm binding was questioned [1], [17]. However, it is possible that their combined complex structures, either than a single chain, are responsible for sperm binding [17].

Nowadays, several proteins besides ZP glycoproteins are believed to participate in the two binding events that take place in sperm-egg interactions [1].

2.1.5. Sperm Proteins Involved in Sperm-Egg Interactions

The ligand of ZP3 present on sperm cells it is still not known, however several potential candidates have been proposed, some of them are listed below.

2.1.5.1. GalT

GalT is present on the surface of human sperm and of several other mammals, which binds to ZP3 through the ZP3 N-acetylglucosamine moiteies. Treating purified ZP3 with N-acetylglucosaminidase to remove GalT binding sites leads to the loss of the binding ability in sperm, implying GalT as a specific substrate of ZP3. In addition, targeted mutations at the *galt* gene, compromising GalT expression and presence in sperm cells, turn these unable to bind to ZP3. Furthermore, after fertilization, ZP3 loses the binding sites for GalT, coinciding with the loss of binding activity of this glycoprotein in fertilized oocytes. This may result from the polyspermy blockage mediated by cortical granules release, since they have high levels of N-acetylglucosaminidase. Finally, spermatozoa overexpressing GalT have higher rates of G-protein activation and thus, acrosome exocytosis. However, information is controversial as some reports show that GalT null mice are still able to bind to the zona pellucida, even if at a lesser extent, highlighting the hypothesis that N-acetylglucosamine, on eggs, is not the only molecule involved in egg-sperm interactions [41]. Alternatively, it was also hypothesized that the binding between the oocyte and sperm cells could be mediated by a multimeric complex on spermatozoa instead of a single entity [42].

2.1.5.2. A Desintegrin and A Metalloproteinase (ADAM)

Several ADAMs expressed in male mice germ lines have been implicated in fertilization, such as ADAMs 1, 2 and 3. ADAMs were candidate proteins for sperm-egg interactions through their desintegrin (integrin-like) domain that would bind an egg integrin [43]. In addition to the desintegrin domain, ADAMs also have a cystein-rich domain that is followed by an epidermal growth factor repeat, a spacer region, a transmembrane domain and a cytoplasmic tail [44].

Contrary to mice, in human and gorilla, the *adam1* gene is non-functional, presenting deletions, insertions and stop codons. Hence, it was not considered a candidate for zona pellucida binding.

ADAM2 (or fertilin β) is a testis specific protein thought to be involved in sperm-egg interaction [44]. In fact, knocking out ADAM 2 severely compromises sperm-egg binding in mice. Unexpectedly, the deletion of one ADAM resulted in loss of several others, which suggests inter-dependency on the regulation of their surface expression [43]. In humans, ADAM 2 was shown to bind integrin $\alpha_6\beta_1$ on the oolema, mediating sperm-egg interactions [45]. Furthermore, an inhibitory study using antibodies demonstrated another protein interacting with ADAM 2 in mouse eggs: integrin $\alpha_9\beta_7$. Humans also express this integrin. These results support a role of ADAM 2 in sperm-egg interactions [46].

ADAM 3, also known as cyritestin, is a testis specific metalloproteinase localized in the equatorial region of mice mature sperm cells [41], [44]. The equatorial region corresponds to the portion of the plasma membrane involved in the initial contact between sperm and oocytes during binding and fusion [44]. Targeted deletions of this metalloproteinase resulted in normal sperm migration but compromised binding to the zona pellucida [41]. Despite its possible role in fertilization in mice, in humans ADAM 3 is a pseudogene, being unable to be involved in sperm-egg interactions [44].

Noticeably, structure-function data suggests that ADAMs could have redundant roles, explaining the conflicting data from knock out studies [43].

2.1.5.3. Zonadhesin

Zonadhesin was isolated from pig sperm membranes in 1994 by Hardy and Garbers and was associated with species-specificity [47]. It remains the only mammalian protein having a validated role in species-specificity. It is produced during spermatogenesis and located in the outer acrosomal membrane of spermatozoa. In humans, it is only detected in capacitated sperm cells and becomes undetectable after acrosome reaction. Zonadhesin shares a common structure that is conserved between species; however it is highly variable in amino acid sequence. Sperm competition studies show that spermatozoa from zonadhesin-null mice were able to bind to the zona pellucida of other mammalian species such as pig and rabbit, corroborating previous observations. Targeted mutation to zonadhesin did not alter sperm morphology or physiology with only

species-specificity being compromised. Of note, proteolytic activity and glycosylation are involved in zonadhesin differences between species [47].

Since the exposure of zonadhesin occurs after capacitation, this supports a recent model for sperm-zona pellucida interactions, in which acrosomal proteins influence sperm-oocyte binding [47].

2.1.5.4. IZUMO

Izumo was named after a Japanese marriage shrine. This gene encodes for an immunoglobulin (Ig) type I membrane protein with one extracellular Ig domain. Recently, the IZUMO family was found to have four members (IZUMO 1 to IZUMO 4). Near the N-terminus, after the signal peptide and before the Ig domain, there is a sequence of high degree of homology between the IZUMO members, being designated by the 'IZUMO domain'. During the acrosome reaction, IZUMO translocates from the anterior head of the sperm to the site were fusion occurs [48]. The Ig domain of IZUMO 1 has the ability to form dimmers and, in fact, complexes of IZUMO 1 and IZUMO 3 were reported in sperm. Despite having a well-conserved glycosylation site in the Ig domain, glycosylation was considered dispensable for IZUMO 1 function, although it provided protection against its fragmentation in the epididymis [48]. IZUMO 1 knock out studies in mice showed that it is essential for sperm-egg interactions [46]. IZUMO null mice were healthy and had no development abnormalities; males were sterile but exhibited normal mating behaviour, and their sperm penetrated the ZP but did not fuse with the oocyte. This lead to accumulation of spermatozoon in the perivitelline space [48].

2.1.6. Oocyte Proteins Involved in Sperm-Egg Interactions

Besides ZPs, there are other proteins of the oocyte that are thought to interact with proteins on sperm cells surface.

2.1.6.1. Integrins

Integrins are heterodimeric transmembrane proteins involved in cellular adhesion [46], [49]. There are 18 α and 8 β subunits, forming 24 different proteins, which are divided into five families [46]. Expression of integrin is considered crucial

in the early stages of development [50]. In addition, one integrin is able to bind more than one ligand. Integrins are not just involved in cellular adhesion but also participate in cell signalling, regulating intracellular pH, intracellular Ca^{2+}, inositol lipid turnover and protein phosphorylation [51]. After integrin-stimulated adhesion, several intracellular pathways are activated, such as MAPK (mitogen-activated protein kinase) and PI3K (phosphatidyl-inositol 3-kinase) pathways, involved in oocyte activation [51]. Integrin-mediated adhesion or ligand binding can be influenced by several factors, including ligand avidity [49].

The role of β1 integrin in fertilization remains controversial [49]. Adhesion and inhibition studies suggest that β1 integrin on eggs interacts with ADAM 2 on sperm [52]. β1 integrin was first reported to increase sperm cells binding rate but to be dispensable for sperm-egg fusion and not required for initiation of polyspermy blockage [52]. However, others report a significant decrease of sperm-oocyte fusion after cell treatment with monoclonal antibodies against β1 integrin. In addition, it has also been reported the co-localization of β1 integrin oolemal patches with fused spermatozoa [49]. Kinetic studies of sperm cell binding from WT and β1 null mice imply that β1 integrin helps sperm-egg adhesion. This step can be bypassed by attachment to other proteins in a binding-fusion complex [52].

2.1.6.2. CD9

CD9 is a β1-integrin-associated tetraspanin ubiquitously expressed [48]. Tetraspanins are surface proteins composed of four transmembrane domains and are able to form complexes with each other and with other membrane proteins, forming a “web of tetraspanins”. They can also regulate the molecules with which they interact [49]. Blocking antibodies against this protein have been shown to inhibit sperm-binding and fusion with ADAM 2 [44]. CD9 knockout mice are healthy but females are infertile. CD9 null eggs were unable to fuse with sperm, but since they could still bind to the zona pellucida, this resulted in accumulation of sperm in the perivitelline space [48]. Rescue experiments, using wild-type and mutant CD9 mRNA, have highlighted the importance of its large extracellular loop in sperm-egg fusion [53]. A large extracellular loop of CD9 was shown to inhibit fusion when pre-incubated with eggs, but not with sperm cells, implying that CD9 was not a sperm

receptor. Since CD9 is able of interacting with several proteins, it was thought that it could be modulating the function of a sperm receptor [49]. Overall, these results imply CD9 as crucial for sperm-egg fusion [44].

A scheme with proteins known to be involved in sperm-egg interaction is presented in Figure 6; however, other unreported proteins may be involved in these mechanisms, such as APP.

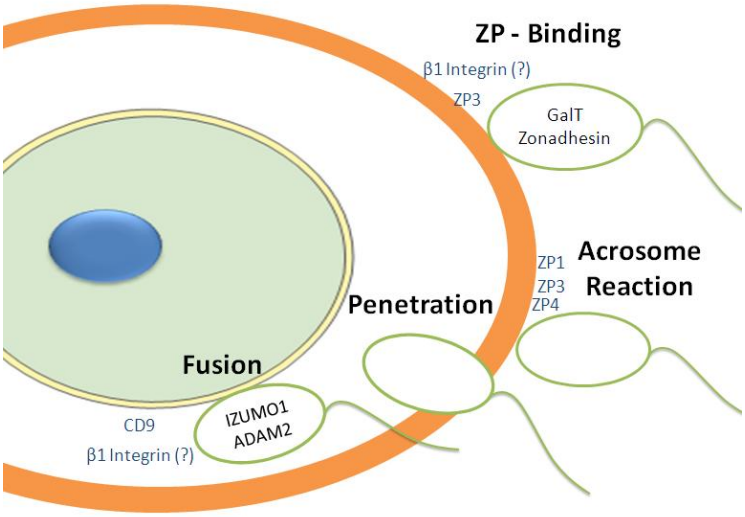

Figure 6. Representation of sperm-egg interactions. Egg proteins believed to interact with sperm at different stages are in grey.

2.2. Alzheimer's Amyloid Precursor Protein (APP)

Alzheimer's disease (AD) is a multifactorial neurodegenerative disease and the most common cause of dementia [54], [55]. AD is classified into early onset (before 65 years of age) and late onset (after 65). The first is also known as Familial AD and follows the Mendelian inheritance pattern, with several genes being involved, such as *app*, *presenilin 1* (*psen 1)* and *presenilin 2 (psen* 2). Mutations in these genes result in amyloid beta (or abeta, Aβ) production leading to neuron loss and dementia. The late onset forms have also several genes associated that give a predisposition for AD, such as *apoe*, in which the allele ε4 in homozygosity is the main risk factor, probably through a change in the protein conformation [55].

AD pathologic features include extracellular deposits of amyloid fibrils designated by senile plaques and intracellular neurofibrillary tangles (Figure 7) of hyperphosphorylated Tau. The main component of amyloid plaques is the Aβ peptide. This amyloid peptide ranges from 38 to 43 amino acids and is derived from a larger protein, the Alzheimer's amyloid precursor protein, APP [54], [56].

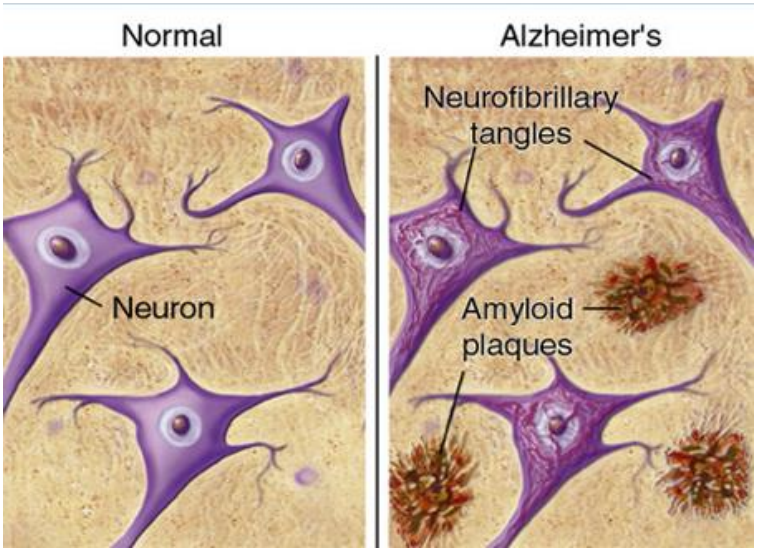

Figure 7. Representation of Alzheimer's pathologic features. Retrieved from BrightFocus Fundation.

APP is a type I transmembrane protein with only one membrane-spanning domain, a large extracellular amino terminus and a short cytoplasmic domain [54]. The extracellular domain is composed of two subdomains (E1 and E2), interconnected by an acidic domain. E1 is divided into growth factor-like domain (GFLD) and copper-binding domain (CuBD) [57]. E2 subdomain consists of two distinct supercoiled substructures connected by a central helix [57]. This protein is ubiquitously expressed in tissues and culture cells. Several functions have been attributed to it, such as in cellular adhesion, heparin-binding, cellular growth, neuronal excitoprotection, proteinase inhibition, neuronal differentiation [56].

2.2.1. APP Proteolytic Processing

APP is cleaved by different proteases designated α-, β- and γ-secretases. Upon cleavage, a large active peptide is formed, the secreted APP (sAPP). sAPP

can be originated by two distinct pathways [54] (Figure 8). The β-secretase pathway has been implicated in the pathogenesis of AD. APP undergoes proteolysis by an aspartyl protease β-secretase 1 (BACE) producing sAPPβ as well as a membrane-bound C-terminal fragment (APP-CTFβ). This is further cleaved by γ-secretase releasing Aβ and the APP intracellular cytoplasmic domain (AICD) [54]. The α-cleavage pathway is the one mainly activated under physiological conditions. α-secretase, which is thought to be a metalloproteinase, such as ADAM10 and ADAM9, cleaves APP within the Aβ-sequence, releasing sAPPα and a membrane-bound CTF (APP-CTFα). The latter is cleaved by γ-secretase, generating a truncated Aβ fragment named p3 and AICD. sAPPα is present is healthy brains and is associated with physiological functions, such as the increase of synaptic density, memory retention, and proliferation of embryonic neural stem cells, being considered neurotrophic and neuroprotective [54].

The APP N-terminus can be also cleaved by another pathway that appears to be modulated by protein kinase C (PKC), generating small N-terminal fragments (NTFs) of approximately 12-30 kDa. These NTFs, found in human blood and CSF (cerebrospinal fluid), appear to play a functional role during neuronal development and/or in adult synaptogenesis. [54].

2.2.2. APP Isoforms

APP has several isoforms resultant from alternative splicing of three exons (7, 8 and 15), generating 8 isoforms (Figure 9) [58]. The isoforms were named according to their amino acid length, with the full length APP being designated APP 770. This isoform encodes a Kunitz protease inhibitor (KPI) domain in exon 7. APP 751 lacks a 19 amino acid sequence in exon 8 that is homologous to MRC OX-2. APP 695 lacks exons 7 and 8, and is the most abundant variant in mammalian brain. The APP-714 lacks only the KPI domain (exon 7) [59].

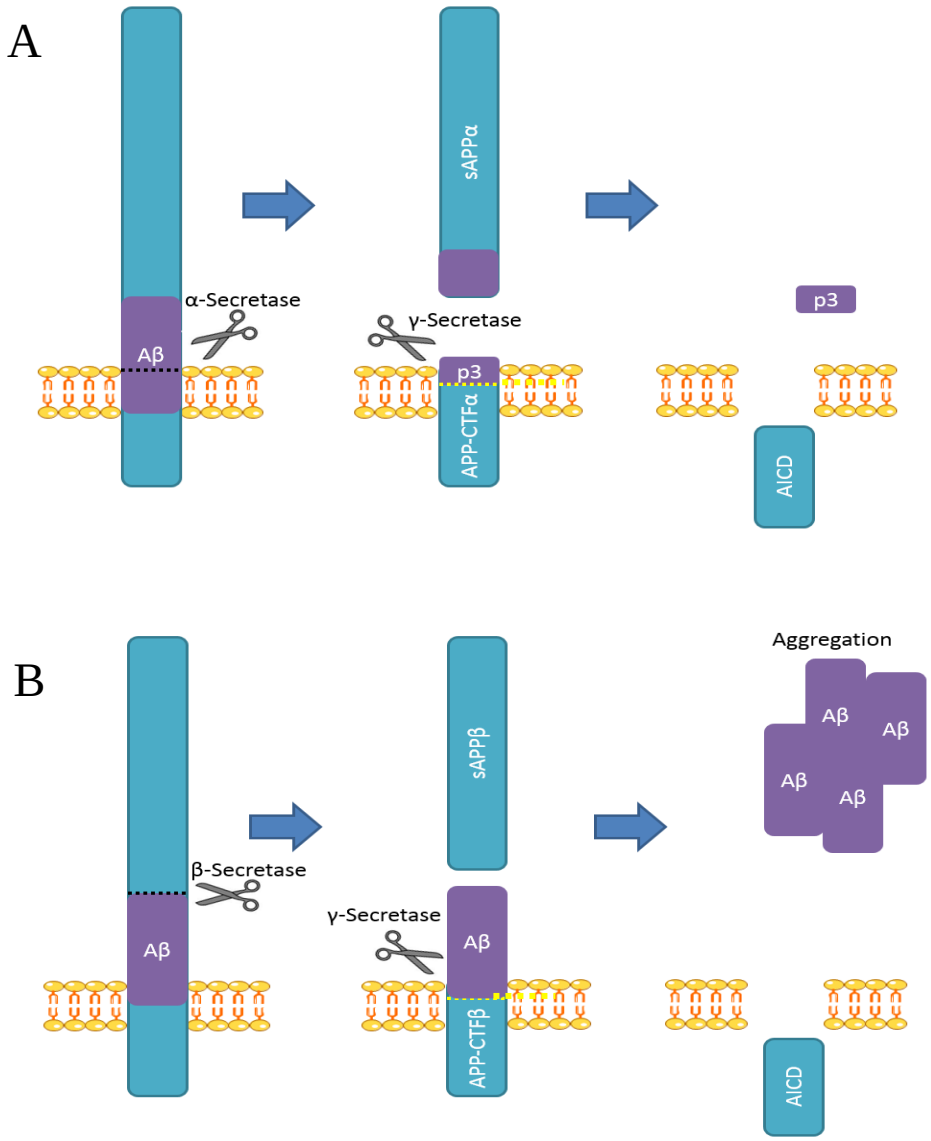

Figure 8. Proteolytic processing of APP. **A.** The α-cleavage pathway. **B.** The amyloidogenic pathway. α- and β-secretase cleavage sites are showed by black dotted lines and γ-secretase showed by yellow dotted line.

Transcripts without the exon 15, which encodes 18 amino acids, were initially found in leukocytes and hence designated L-APP [58]. Four L-APP variants exist (L-APP 752, L-APP 733, L-APP 696 and L-APP 677), which are ubiquitously expressed but quite rare in neurons [59]. The spliced out of exon 15 generates an isoform that binds through a xylose sugar to a serine and forms the core protein of the secreted chondroitin sulfate proteoglycans, termed 'appicans' [60].

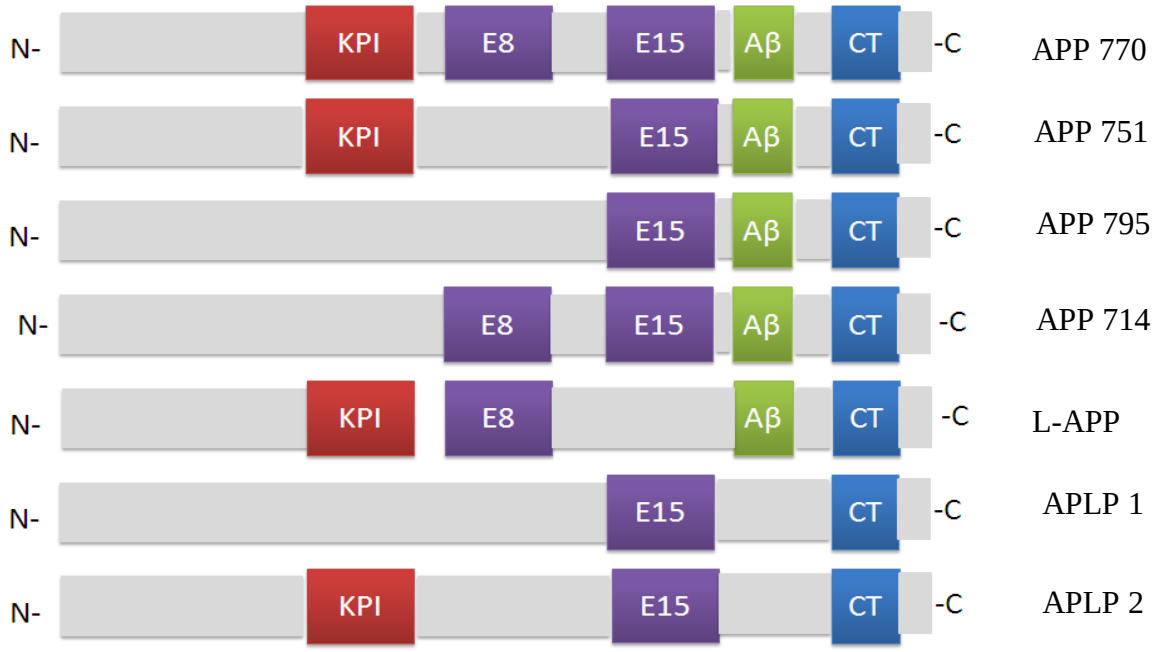

Figure 9. Comparison of the APP isoforms' structure. KPI, Kunitz Protease Inhibitor domain (in E7, exon 7); E8, exon 8; E15, exon 15; CT, cytoplasmic domain.

All these isoforms belong to the APP superfamily, which includes APP-like proteins (APLPs) (Figure 9). The APP closest protein is APLP2, sharing 46% of amino acid sequence (mainly at the protein N- and C-terminus) and, like APP, it is ubiquitously expressed [58], [59], [61]. This protein is encoded by chromosome 11, whereas APP is encoded by chromosome 21. APLP2 is present in humans, rat and mouse, sharing a high homology with APP; however the N-terminus of the transmembrane domain is highly divergent, with APLP2 not including the Aβ sequence. In fact, Aβ is only present in APP and L-APP [58], [59]. APLP2 also lacks APP's exon 8 but has exon 15 present [58]. APLP1 is encoded by chromosome 19, and its expression is confined to the nervous system [61]. It shares 35% of homology with full-length APP (770), and the N-terminus of its transmembrane domain is again the most divergent region from APP. APLP1 has a very similar structure to APLP2 but, contrary to APLP2, APLP1 does not have the KPI domain. Both APLP1 and 2 have several isoforms, also generated by alternative splicing. Knock out studies with null-mice for APLP1 or 2 or double knock out of APP/APLP1 are viable, however knock outs of APP/APLP2 or

APLP1/2 are lethal. These results imply some functional redundancy that is corroborated by structure similarity [61].

2.2.3. APP Dimerization

Studies of APP structure suggest it has receptor-like functions. That led to the hypothesis of APP dimmer formation and, in fact, it was shown that APP undergoes dimerization [61]. The E1 subdomain of APP is the main interface for dimerization [57], [61], and deletion of the E2 domain had no effect on this [57]. The linker between E1 and E2 also appears to be crucial for dimerization through the interaction with E1, allowing its cis- and trans-dimerization (Figure 10) [61]. Furthermore, heparin binding to E1 induces homodimerization of APP [62].

It is also believed that trans-dimerization is associated with cellular adhesion [57], [61]. APP can form homo- and heterodimers between APP, APLP1 and APLP2, which are involved in molecular adhesion through trans-interaction. APP and APLPs are thought to be related to dynamic intercellular processes and the accumulation of APP and APLPs in sites of cell-cell interaction indicated their direct trans-cellular interactions [57]. Furthermore, heterocomplexes of APP family members were found in mice brains, implying a role for cellular adhesion [61]. Surprisingly, reports using transgenic mice showed *in vivo* that the APP/APLP interaction is independent of glycosylation [61]. Noticeably, APP and APLP1 and 2 may have several functions, depending on subcellular location and expression, as well as the formation of homo or heterodimers [57].

Cellular adhesion mediated by molecules such as cadherins is also performed by trans-dimerization [61], and N-cadherin also mediates APP dimerization [62]. β-1 Integrin is also known to bind APP and mediate its role in cell adhesion. Furthermore, it was suggested that a complex of APP and Fe65 could regulate integrin signalling in focal adhesions [63]. A relationship between APP and β1-integrin was also described in the neuritogenesis process [64].

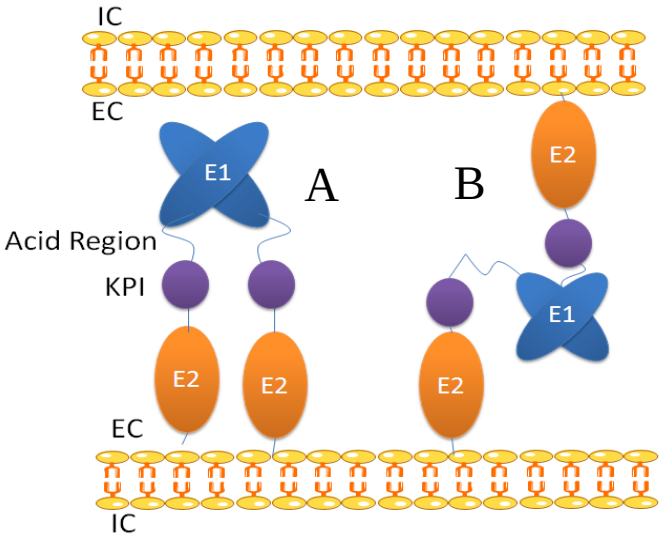

Figure 10. Representation of APP cis (A) and trans-dimerization (B).

2.2.4. APP in Sperm Cells

YWK-II, a truncated form of APLP2, was detected in the equatorial region of the spermatozoon's head, mid-piece and tail. Similarly, APP itself was also found in sperm cells. Blocking antibodies against APLP2 were shown to compromise fertility in female rats by targeting the interactions between sperm and egg [59]. In our laboratory we have shown that full-length APP and/or APLPs are present on the surface of the entire spermatozoon, but with particular abundance on the head (Figure 11) [59]. All this data suggests that the APP superfamily may have a role in reproduction, particularly in sperm interactions with the matrix or the oocyte.

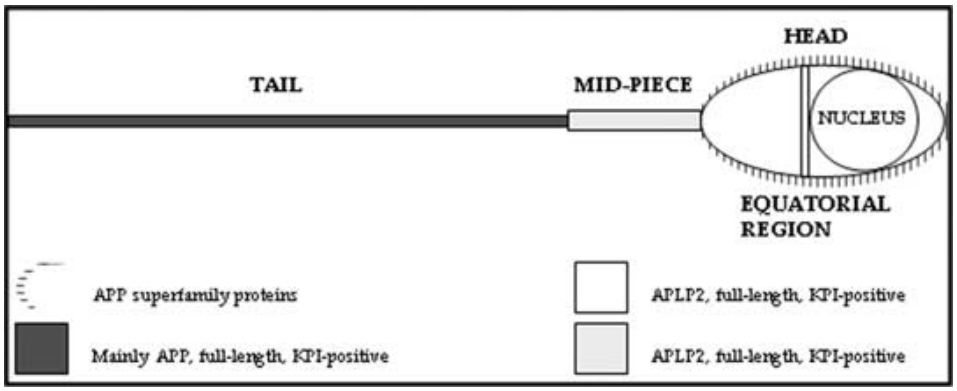

Figure 11. Representation of APP and its isoforms distribution in sperm cells. Taken from Fardilha, M. et al (2007) [59]

3. Aims of This Thesis

Since APP and APLPs are expressed in the plasma membrane of the sperm cell's head, a region involved in sperm-egg interactions, and that ZP3 is the primary sperm receptor, it can be hypothesized that APP may mediate interactions between those cells. Furthermore, both APP and ZP3 are glycosylated and APP undergoes trans-dimerization, implying a role in cellular adhesion, an important process in sperm-egg interactions.

The work here presented aimed to evaluate potential functional and physical relationships between ZP3 and APP. Hence, using different cell lines that endogenously expressed both proteins, several analyses were performed.

Thus, the main objectives were:

- Search for relevant motifs in ZP3 that may relate to APP binding and physiology;
- To evaluate if APP and ZP3 co-function in cell-cell adhesion;
- To observe if ZP3 and APP co-localize in different cells lines;
- To test if ZP3 and APP physically interact.

4. Materials and Methods

4.1. ELM Bioinformatic Tool

"The Eukaryotic Linear Motif resource for functional sites" (ELM) was used to analyse functional motifs present in the ZP3 amino acid sequence. This software is designed for detection of functional motifs within an amino acid sequence and is freely available in (http://elm.eu.org/). Functional sites were detected using regular expressions (patterns) through a logical filter to discriminate between true matches and false positives. This software uses PHI-BLAST to map predictions concerning a specific sequence, and the mapping is performed by sequence similarity and motif conservation. The localization of these sequences has implications for their function. Taking into account that these sequences have to be recognized by other proteins they have to be structurally accessible and in the same cellular compartment. ELM has several filters such as taxonomic range filter, cell compartment filter, structure filter, globular domain filter and the probability filter. This software provides information about functionally relevant sequences, mapping their location, describing them, placing them in a cellular compartment, providing a pattern with an associated probability. Patterns with low probabilities are regarded as regular expressions, whereas those with higher probabilities have a more degenerate expression.

4.2. Cell Culture

4.2.1. Cell Lines and Maintenance Conditions

4.2.1.1. HeLa Cells

In the impossibility of performing sperm-egg interaction assays in our laboratory, immortalized cell lines were used to study the role of ZP3 and APP in cell-cell adhesion. The HeLa mammalian cell line was used, since according to The Human Protein Atlas (www.proteinatlas.org) it has a good expression of endogenous ZP3 and APP, it is a highly adhesive cell line, and is routinely used in the lab. HeLa cells are an immortalized cell line originated from cervical cancer cells. These were originally collected from a cancer patient named Henrietta

Lacks. HeLa cells were maintained in Dulbeco's Minimum Essential Media (DMEM; Gibco) supplemented with 10% foetal bovine serum (FBS; Gibco), 100 IU/mL of penicillin, 100 µg/mL of streptomycin and 25 µg/mL of amphotericin B utilizing penicillin G (Life Technologies). Cells were incubated at 37ºC in 5% Co_2 and were subcultured when 90% confluence was reached.

4.2.1.2. CHO Cells

Chinese hamster ovary cells (CHO-K1; ATCC number: CCL6) were also used due to their ovary nature. CHO were cultured in Ham's F-12 nutrient mixture (Sigma-Aldrich) containing 2 mM L-glutamine, 10% FBS (Gibco), 100 IU/mL of penicillin, 100 µg/mL of streptomycin and 25 µg/mL of amphotericin B utilizing penicillin G (Life Technologies). Cells were incubated at 37ºC in 5% CO_2 and subcultured when 90% confluence was reached.

4.2.1.3. HeLa-CHO co-cultures

When indicated, HeLa and CHO cells were co-cultured at 50-60% confluence in six-well plates (immunocytochemistry assays), or at 100% confluence in 100 mm plates (immunoprecipitation assays), in the CHO cells medium.

4.3. Antibodies

The primary antibodies used in this work were the polyclonal ZP3 rabbit antibody from Proteintech (21279-1AP), the monoclonal 22C11 anti APP N-terminus mouse antibody (Chemicon), directed against APP N-terminus, the polyclonal anti-APP CT695 (Invitrogen) directed against APP C-terminus, and antibodies against beta1-Integrin: total beta1-Integrin MAB1981 antibody (Millipore) and a function blocking beta1-Integrin MAB1959 antibody (Millipore).

Polyclonal ZP3 rabbit antibody recognizes the N-terminus of human ZP3 and detects several glycosylated forms of this protein (e.g. 47kDa and ≈ 92kDa). The 22C11 and CT695 APP antibodies both recognize full length APP O- and N- and O-glycosylated forms (≈100kDa and 130kDa).

Table 1. List of antibodies used in cell-cell adhesion (CCA), immunocytochemistry (ICC), immunoprecipitation (IP), and western blot (WB) assays, with respective dilutions.

Name	Epitope	Assay	Secondary Antibody
ZP3	N-terminus of ZP3 (52-251 aa)	CCA (1:100) ICC (1:100) IP (1:1000), WB (1:500)	Horseradish Peroxidase conjugated (1:5000) or Fluorophore-conjugated (1:300) α-Rabbit IgGs
22C11	N-terminus of APP	IP (1:20), WB (1:250), ICC (1:50)	Horseradish Peroxidase conjugated (1:5000) or Fluorophore-conjugated (1:300) α-Mouse IgGs
C-Ter	C-terminus of APP	IP (1:100)	-
Beta1-Integrin MAB1959	*non described*	CCA (1:100)	-
Beta1-Integrin MAB1981	Beta1 Integrin 588-706 aa sequence	ICC (1:100)	Fluorophore-conjugated (1:300) α-Mouse IgGs

4.4. Cellular Adhesion Assays

4.4.1. Optimization of CHO-HeLa Cells Adhesion Assays

Cell-cell adhesion assays were undertaken based on Zepeda-Moreno et al (2011) [65]. In a 96-well plate, a feeder layer of 15 000 HeLa cells was plated and incubated overnight at 37ºC in 5% CO_2. In the following a day the feeder layer had reached confluence. Then, different number of HeLa and CHO cells (between 10^4 and 10^5 cells, indicated in each assay) were plated over the feeder layer or directly on the plate plastic bottom. Following, plates were incubated for 1h at 37ºC in 5% CO_2, after which the plate was inverted and cells incubated for 1,5 hours at 37ºC in 5% CO_2. Then, with the plate tilted at 45-70 degrees, the non-adherent cells in the supernatant were collected with a micropipette to an empty 96-well plate. With an end-volume of 100 µL of cells, 10 µL of resazurin (0.1 $mg.mL^{-1}$ resazurin in phosphate buffer saline (PBS) [Pierce, Perbio, Thermo Scientific, Bonn, Germany]) were added and incubated overnight at 37ºC in 5% CO_2. In the following day cells were indirectly evaluated via the spectrophotometrically

quantification (at 570 and 600 nm) of the conversion of resazurin to resorufin by metabolically active cells using the Infinite M200 microplate reader (Tecan). A final optical density (O.D.f) was determined for each sample: (O.D.570/O.D.600)-(O.D.570c/O.D.600c); 'c', O.D. of control samples (medium only plus resazurin).

4.4.2. Antibody Interference Assays

In a 96-well plate, following the protocol described by Zepeda-Moreno [65], a feeder layer of 15 000 HeLa cells per well was plated and incubated overnight at 37ºC in 5% CO_2. In the following day, the cells in the feeder layer were confluent.

Before seeding, the top and/or the bottom (feeder) layer were treated with specific antibodies against APP, ZP3 or beta1-integrin. Top layer: CHO cells were washed with PBS, collected, and counted in a haemocytometer using Trypan blue as a vital dye. Cells were centrifuged for 3 min at 1000 g, and ressuspended in 100 μl of 3% BSA in PBS in a sterile microtube. The respective blocking antibody (Table 1) was added, and cells incubated for 1h at 4º C, with orbital agitation. Cell medium was added, and cell number-normalized aliquots were plated as described above. The experiments were performed in triplicate.

4.5. Immunocytochemistry (ICC) Assays

To determine if ZP3 and APP co-localize in mammalian cells and their sub cellular localization, immunocytochemistry assays were performed in CHO cells cultures, HeLa cells cultures, and in CHO-HeLa cells co-cultures. The co-localization of ZP3 with beta1-Integrin was also evaluated.

On a 6-well plate, HeLa cells, CHO cells, or a HeLa-CHO co-culture were plated on coverslips and cultured until 50-60% confluence at 37ºC in 5% CO_2. Cells were washed twice with PBS and fixed in 4% paraformaldehyde in PBS for 20 minutes. Following, cells were washed with PBS three times, 10 minutes each. After removal of the PBS, cells were permeabilized with 0,2% TRITON in PBS solution at room temperature (RT) for 10 minutes. Cells were washed three more times with 1x PBS for 10 minutes each. Then, these were blocked in a 3%BSA/PBS solution for 30 minutes at RT and then washed with PBS for 5

minutes. Cells were incubated with the anti-ZP3 and anti-APP 22C11 primary antibodies (respective dilutions are present in Table 1) for two hours and then washed three times with PBS for 10 minutes each. The secondary antibodies anti-rabbit Alexa Fluor 594® (1:300; Molecular Probes®, Life Tecnhologies) and anti-mouse Alexa Fluor 488® (1:300; Molecular Probes, Life Technologies) were incubated with the cells for 1 hour in the dark. The coverslips were further washed three times with PBS and one last time with distilled water, and then mounted with the DAPI-plus VECTASHIELD® mounting media (Vector Laboratories) on 0.1 mm microscope glass slides for epifluorescence (Olympus IX-81 motorized inverted microscope) and confocal microscopy analyses [LSM 510 META confocal microscope (Zeiss, Jena, Germany; equipped with an Argon laser of 488 nm (green channel), a 561 nm DPSS laser (red channel) and a Diode 405-430 laser (blue channel)].

4.6. Immunoprecipitation (IP)

To determine if ZP3 and APP physically interact, immunoprecipitation assays were performed. Plates of 100 mm of confluent cultures of HeLa cells, alone or co-cultured with CHO cells, were used. The antibodies used were the anti-ZP3 and the anti-APP CT695 antibodies (dilutions used are in Table 1).

When indicated, a crosslinker solution with dithiobis(succinimidyl propionate) (DSP; Thermo Scientific) was used to stabilize the interaction. In these assays, the cells medium was aspirated, cells were washed two times with PBS, and 750µl-1 ml DSP cross linker (0.4 mg DSP/ml PBS) was added and cells incubated for 45 min at RT. After adding the crosslinker, cells were placed on ice and washed with a solution of PBS and PMSF (diluted 1:100). Cells were further collected from the 100 mm plates with plastic scrappers (Greiner) into microtubes. All samples were centrifuged at 3000 g for 5 minutes at 4 ºC. After removing the supernatant, 600 µL of lysis buffer was added to each sample. During the 30 minutes of lysis, lysates were for three times pipetted up and down to ensure proper cellular lysis. In the meantime, magnetic beads coupled with sepharose G (dynabeads from Life Technologies, or magnetic beads from Millipore) were

washed in 3% BSA/ 1% PBS three times and kept in the same solution. After cellular lysis, the samples were centrifuged at 20 000 g for 5 minutes at 4 ºC, and the supernatant was collected. To an aliquot of 40 µL of the lysates supernatant, 5 µL of 10% SDS (sodium dodecyl sulphate) and 15 µL of 4x loading buffer (LB) were added, and the aliquots boiled at 90ºC for 10 minutes and kept at 4ºC. The remaining supernatant sample was pre-cleared by incubation with 9 µL of beads for 1 h at 4 ºC with orbital agitation. To each pre-cleared supernatant, 30 µL of the pre-washed sepharose G bead were added, together with the respective antibodies (antibody dilutions are present in table 1). The immunoprecipitation was left to occur overnight at 4ºC with orbital agitation.

On the following day, the microtubes were placed on the magnet and the supernatant was discarded. The beads were first washed with 500 µL of a 3%BSA/1x PBS solution, with orbital agitation for 5 minutes at 4ºC. The microtubes were placed again on the magnet, the washing buffer (supernatant) was discarded, and the beads washed four times with PBS, for 10 minutes each, with orbital agitation at 4ºC. After removing the last supernatant, 100 µL of LB/1%SDS was added. The samples were then boiled at 90ºC for 10 minutes prior to being subject to western blot. The experiments were performed in duplicate.

4.7. Western Blot Assays

After the IP assays, lysates and IPs were subjected to 6.5 or 7.5% sodium dodecylsulfate polyacrilamide (SDS) gel electrophoresis (PAGE), after which the resolved proteins in the gel were electrotransferred onto nitrocellulose membranes. After transfer, membranes were hydrated in 1x TBS for 10 minutes, and blocking solution was added for 1h (5% non-fat dry milk in 1x TBS-T), to block non-specific binding sites. Primary antibody, diluted in 3% non-fat dry milk in 1x TBS-T, was added and incubated with membranes overnight. The membranes were further washed three times with 1x TBS-T for 10 minutes each, after which they were incubated with the respective secondary antibody, diluted in 3% non-fat dry milk in 1x TBS-T, for 2h with agitation. All antibody dilutions are present in table 2. Membranes were finally washed three times with 1x TBS-T for 10 minutes each.

The detection of the secondary antibody was carried out using the enhanced chemiluminescence (ECL) detection method. After the washes, membranes were incubated with 1 mL of Luminata™ Crescendo (Millipore) for 3-5 minutes. Inside a dark room, sheets of Hyperfilm ECL (GE Healthcare) were placed over the membranes in an x-ray cassette. After the appropriate time of exposure, the film was developed in a developer solution (Sigma Aldrich), washed in water and fixed in a fixation solution (Sigma Aldrich). Membranes were then washed three times with 1x TBS-T and left to dry. The films were scanned in a GS-800 calibrated imaging densitometer (Bio-Rad) and bands were scanned using Quantity One Software (Bio-Rad).

5. Results

5.1. *In Silico* Characterization of ZP3 Functional Motifs

The functional motifs of the ZP3 amino acid sequence were first analysed using the “Eukaryotic Linear Motif” (ELM) bioinformatics tool, to unravel potential motifs involved in binding to APP or to known APP binding partners, or motifs involved in pathways common to APP.

After entering the human ZP3 amino acid sequence, the software displayed results for globular/ transmembrane domains and signal peptide length detected using SMART (Simple Modular Architecture Research Tool) tool. The provided signal peptide is composed of 19 amino acids, very similar to the 22 reported in the literature. Similarly, the ZP domain proposed has 258 amino acids (45-303), also very close to the published results (45-304) [29].

5.1.1. ZP3 Cleavage Sites

ELM found three ZP3 cleavage sites: N-arginine dibasic convertase (NDR) cleavage site, furin cleavage site and proprotein convertase 1 (PCSK 1) cleavage site (Figure 11).

NRD Cleavage Site

NRD convertase is a metalloendopeptidase of the M16 family involved in protein processing. It can be found extracellularly, at cell surface or in the Golgi apparatus. This enzyme cleaves proteins at the N-terminus of arginine (Arg) residues in dibasic motifs (Arg-Arg or Lys-Arg). It has been shown to cleave α-neoendorphin, dynorphin, preproneurotensin and somatostatin. This enzyme has two isoforms, NRD 1 and NRD 2. They differ on a 68 aa sequence close to the active site present only in NRD 2, which can have implications in its function. Northern blot analyses have shown that NRD 2 represents 50% of transcripts in human testis. It can also be found in the cytoplasm of elongated spermatids and has been associated with sperm cell differentiation during spermatogenesis [66]. Besides those tissues, NRD was present in brain cortex of rats [67].

ELM found two regions in ZP3 potentially recognized by NRD 1 convertase: RRQ (334-336) and RRH (351-353). Both sequences have a low probability (approximately 0.007) for the same pattern (.RK)|(RR[^KR]). This patter implies that for the first position any amino acid is allowed, in the second an arginine is present and in the third a lysine; or in the first two positions arginines are present but in the third either a lysine or an arginine are not allowed (see table 2 for the characters used to describe the motifs' patterns).

Table 2. List of characters present in patterns detected by ELM (Adapted from elm.eu.org)

Character	Name	Meaning
.	Dot	Any amino acid allowed
[...]	Character Class	Amino acids listed are allowed
[^…]	Neglected Character Class	Amino acids listed are not allowed
(min, max)	Specific range	min, required; max, allowed
|	Alternation	Matches either expression it separates
()	Parenthesis	Used to mark separate parts of the expression

Furin Cleavage Site

Furin is a serine endoprotease and a member of the subtilysin-like family, which is a family of pro-protein convertases. Similar to NRD, furin also cleaves dibasic residues of precursor proteins. Furin is can be found extracellulary, in the Golgi apparatus and at the membrane. Furin consensus cleavage site is present in growth factors and receptors, serum proteins and viral envelop proteins [68].

The software found one sequence in ZP3 identified by furin, RNRRH (349-353), what may occur extracellularly, in the Golgi apparatus and membrane. The proposed pattern is R.[RK]R. with a probability of approximately 0.0005. The first position has an arginine, the second allows any amino acid, the third allows either arginine or lysine, the fourth has an arginine, and the last allows any amino acid. Furin also recognizes similar sequences in other proteins, such as glycoproteins in viral envelopes of Ebola and Human T-cell leukemia virus 2 (HTLV-2).

Subtilisin/Kexin-Isozyme 1 (SKI 1) Cleavage Site

Like furin, SKI 1 is an endoprotease and member of the subtilisin-like family. SKI 1 is also involved in protein processing at basic residues. This enzyme can be found in the lumen of the endoplasmic reticulum, in the Golgi and extracellularly [69]. SKI 1 is involved in the proteolytic processing of several proteins such as viral proteins of Hepatitis C virus (HCV) that control cholesterol metabolism [70].

ELM showed a motif in ZP3 identified by SKI 1: RHVTE (352-356). The pattern proposed for this sequence was [RK].[AILMFV][LTKF]. with a probability of approximately 0.007. The pattern allows either an arginine or a lysine for the first position; in the second any amino acid is allowed, in the next alanine, isoleucine, leucine, methionine, phenylalanine and valine; in the fourth, leucine, threonine, lysine and phenylalanine are allowed.

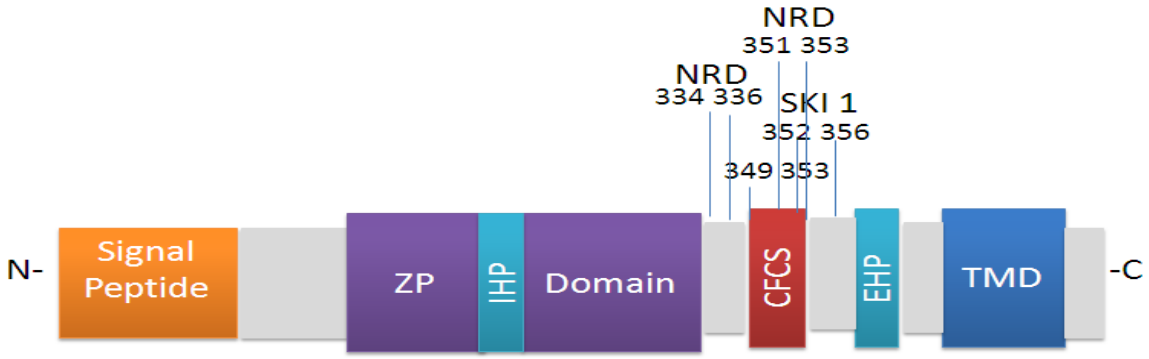

Figure 12. Representation of ZP3 cleavage sites, showing both sites recognized by NRD, one site recognized by SKI 1 and one site recognized by furin (in red).

5.1.2. ZP3 Binding Motifs

This software identified two binding motifs in ZP3: USP 7 binding motifs and WW binding motifs.

USP 7 Binding Motif

USP 7 is a deubiquitinating enzyme, also known as HAUSP. It has four domains, a N-terminus domain, a catalytic domain and two C-terminal domains. This enzyme cleaves ubiquitin from substrates, preventing protein targeting to the proteasome for degradation and increasing the pool of free ubiquitin trough

ubiquitin recycling. USP 7 is present in the nucleus and mediates deubiquitination of P53 and Mdm2 [71].

ELM reported three motifs in ZP3 recognized by USP 7: PETSV (35-39), PSNSW (305-309) and PSHSR (330-334). The associated pattern has a probability of approximately 0.01 for [PA][^P][^FYWIL]S[^P], in which the first position allows a proline or an alanine, the second excludes proline, the third excludes phenylalanine, tyrosine, tryptophan, isoleucine and leucine; the fourth position has a serine and the last position only excludes proline.

Besides ZP3, other proteins have a USP 7 binding motif, such as human Mdm2 and human p53, corroborating previews publications [71]. Additionally, human Mdm4 was also proposed by ELM to share a USP 7 binding motif.

WW Binding Motif

WW domains are named after the two tryptophan residues crucial for their activity, and consist of small regions of 38 to 40 amino acids in a β-sheet [72]. This module is one of the smallest that is able to fold as a monomer without disulfide bonds or cofactors. Proteins with this domain are divided into two major and two minor groups: Group I, one of the major groups, binds polypeptides with the consensus sequence PPxY; Group II, also a major group, bind peptides with PPLP motif; the third group binds to proline-rich motifs flanked by R or K and the last group (IV) binds to short phosphoserine or phosphothreonine followed by a proline [73]. Proteins with this motif are involved in protein-protein interactions trough binding of proline rich motifs. In addition, this domain also plays a role in cell signalling [72]. In the nucleus it was shown to participate in the co-activation of transcription and modulation of RNA-polymerase II activity. The WW domain has been implicated in several human diseases, including AD [73].

ELM found one WW domain motif, DCGTPS (326-331) and proposes that binding to this motif occurs in the cytosol and in the nucleus, as referred in the literature [73]. The pattern ... [PV]..P has a probability of approximately 0.02, in which the first three positions allow any amino acid, the following allow only a proline or an arginine the next two allow any amino acid and the last has a proline (see table 3). The WW domain motif was also found in several other proteins in humans besides ZP3, such as α-globin transcription factor, synphilin 1, p53, p73

and beta-catenin. This motif is also present in Fe65, which is binds the cytoplasmic domain of APP, interfering with its the proteolytic processing, regulating the function and availability of APP at cell surface [63].

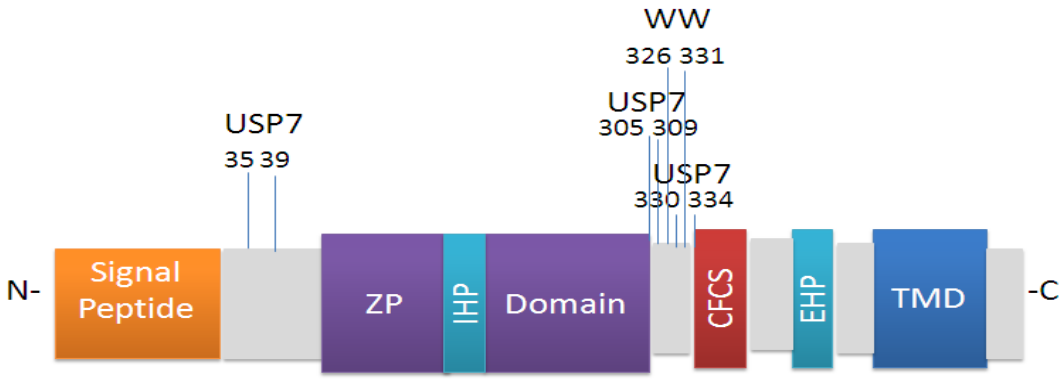

Figure 13. Representation of ZP3 binding motifs, three USP7 binding motifs are highlighted as well as one WW binding motif.

5.1.3. ZP3 Ligand Motifs

ZP3 has a ligand motif recognized by SH3 domains and a TRAF2 binding consensus motif.

SH3 Ligand Motif

SH3 (Src homology 3) domains are small modules of approximately 50-60 residues. This domain usually binds proline residues and is involved in protein-protein interaction, cytoskeleton rearrangement, membrane traffic and organelle assembly.

The software found a sequence on ZP3 for SH3 domain WFPVEGP (309-315) and suggests that ligand binding to this domain occurs in the plasma membrane, focal adhesion and/or cytosol. The pattern ...[PV]..P had an approximate 0.01 probability, where the first three positions allow any amino acid, the fourth is either a proline or a valine the following two allow any amino acid and the last has a proline (see table 3). The sequence present on ZP3 was also found in p73, T-cell antigen CD2, dystroglycan and Tau protein in humans, the latter being an important protein in AD.

TRAF2 Binding Motif

Tumour necrosis factor receptor-associated factors (TRAFs) belong to a family of adaptor proteins which share a common domain in the C-terminus. This region allows interaction with cell receptors and other molecules. TRAF has several isoforms. TRAF2 is a 56 kDa protein and is involved in protein-protein interactions and in cell signalling, playing a role in NF-ΚB activation [74].

ELM reported a TRAF2 binding motif in ZP3: PGQE (368-371). The binding of TRAF2 was reported to occur in the cytosol. The pattern [PSAT].[QE]E has a probability of approximately 0.004, the first position has a proline, a serine, an arginine or a threonine; the second position allows any amino acid, the third has a glutamine or a glutamate and the last position has a glutamate. This motif was also found in other proteins, such as TNF 9, CD 27 and TNF 8.

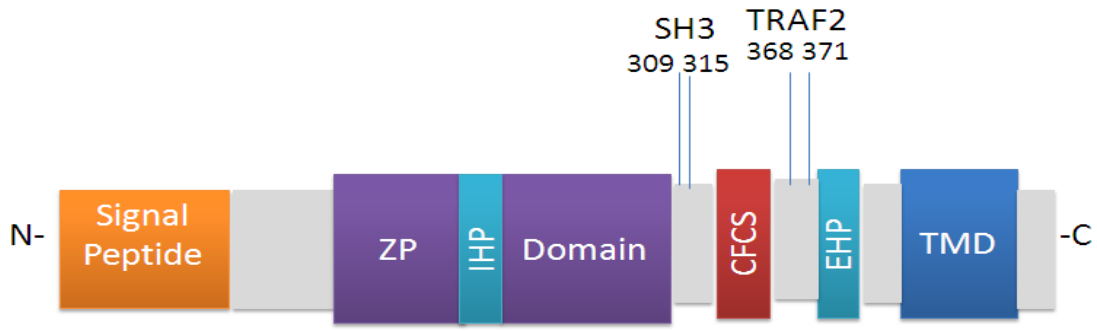

Figure 14. Representation of ZP3 ligand motifs. SH3 and TRAF2 binding motifs are shown

5.1.4. ZP3 Modifications

ZP3 undergoes post-translational modifications, such as phosphorylation and glycosylation. ELM reported several sites in ZP3 that are recognized by several enzymes: CK1 and CK2 phosphorylation sites, glycosaminoglycan attachment site, GSK3 phosphorylation sites, PIKK phosphorylation site, PLK phosphorylation sites and proline-directed kinase phosphorylation site.

CK1 and CK2 Phosphorylation Sites

Casein kinase 1 (CK1) and 2 (CK2) belong to a family of serine/threonine protein kinases involved in signal transduction pathways in a wide range of organisms, from yeast to humans. The CK1 family in humans is composed by seven enzymes, which play an important role in Wnt signalling, circadian rhythms, nucleo-cytoplasmic shuttling of transcription factors, DNA repair and transcription and glycogen metabolism [75]. CK1 is ubiquitously expressed and has been associated with several diseases, including AD, where it has been proposed as a candidate kinase in tau hyperphosphorylation [76]. CK2 is involved in cell growth and proliferation as well as suppression of apoptosis. This enzyme can use both ATP and GTP as a substrate and its main determinant is its specificity towards a negative charge three positions after the modification residue. Knock out studies in mice emphasized the importance of CK2 for cell survival [77].

ELM found one phosphorylation site for CK1 in ZP3: SQWSTSA (341-347) and another for CK2, GGASHPE (30-36). Both kinases can be found in the nucleus and in the cytosol and CK2 can also be present in the CK2 complex. The software found the pattern S..([ST])... with a probability of approximately 0.02 for CK1 and for CK2 the pattern ...([ST])..E with a probability of approximately 0.01. In the first case, the first position is a serine, the following two allow any amino acid, the fourth allows either a serine or a threonine and the last three allow any amino acid. The second pattern allows any amino acid for the first three positions, the fourth allows a serine or a threonine, the following two positions allow any amino acid and in the last position is a glutamate. The sequence corresponding to the CK1 phosphorylation site was also found in two other human proteins: p53 and YAP1. The sequence recognized by CK2 present on ZP3 is also present in human PTEN, DNA repair protein XRCC1 and HIV1.

Glucosaminoglycan Attachment Site

Glucosaminoglycans are polysaccharides involved in physiological functions, such as blood coagulation, cell growth, communication, and morphogenesis [78]. These are ubiquitously expressed in mammals and their sulfation pattern has severe implications in their ability to interact with other molecules [78], [79].

ELM reported one glucosaminoglycan attachment site: TSAS (345-348), with this binding occurring in the Golgi apparatus or extracellularly. The pattern found was [ED] {0,3}.(S)[GA], with a probability of approximately 0.02, where the first position allows a glutamate or an aspartate with a maximum of three of these residues, the second position allows any amino acid, the third has a serine and the last allows a glutamine or an alanine. Proteoglycans with glucosaminoglycan moieties are very important in the extracellular matrix (ECM), since besides structural properties, the addition of these moieties enables the proteoglycan to exert space-filling and lubrication functions in the matrix. Furthermore, the binding functions ascribed to proteoglycans is thought to be involved in the regulation of protein complexes in the ECM [80].

GSK3 Phosphorylation Site

Glycogen synthase kinase 3 is a constitutively active serine/threonine kinase that is ubiquitously expressed, with high levels of expression in the brain. It is involved in cellular metabolism, cell cycle regulation, gene expression, development and neuroprotection. GSK3 has a wide variety of substrates, such as glycogen synthase and β catenin. This kinase has been implicated in the pathogenesis of several diseases, like AD, diabetes, cancer, and inflammation [81]. Noteworthy, the AICD fragment of APP is known to bind Fe65 and, upon their nuclear targeting, to enhance gsk3β expression [82].

ELM found five GSK3 phosphorylation sites in ZP3: GGASHPET (30-37), DCGTPSHS (326-333), HVMSQWST (338-345), SQWSTSAS (341-348) and ADVTVGAT (358-365). Phosphorylation of ZP3 can occur in the cytosol and in the nucleus. The pattern ...([ST])...[ST] has an approximate probability of 0.03. The first three positions allow any amino acid, the forth allows for either a serine or a threonine, the following three allow any amino acid and the last allows a serine or a threonine. The sequence found by the software is also present in many other human proteins, such as p53, ataxin 3, zinc finger protein SNAI 1, SMADs 1 and 3, MYC.

MAPK Phosphorylation Site

Mitogen-activated kinases (MAPK) are essential players in signal transduction networks. These kinases recognize serine/threonine residues

followed by a proline. Dysregulation of MAPK pathways are associated with diseases such as cancer, developmental diseases, neurodegenerative diseases and metabolic diseases [83]. An APP-MAPK relation is currently being investigated in our laboratory (data not published).

ELM found one MAPK phosphorylation site in ZP3: DCGTPSH (326-332). Phosphorylation of ZP3 by MAPK can occur in the nucleus and in the cytosol. The pattern ...([ST])P.. was found with a probability of approximately 0.02. The first three positions allow any amino acid the fourth allows either a serine or a threonine, the following has a proline and the last two allow any amino acid. The short motif found by ELM is present in many other proteins, such as the human retinoic acid receptor α, transcription factors ETV6 and SP1, Myc and HIF1.

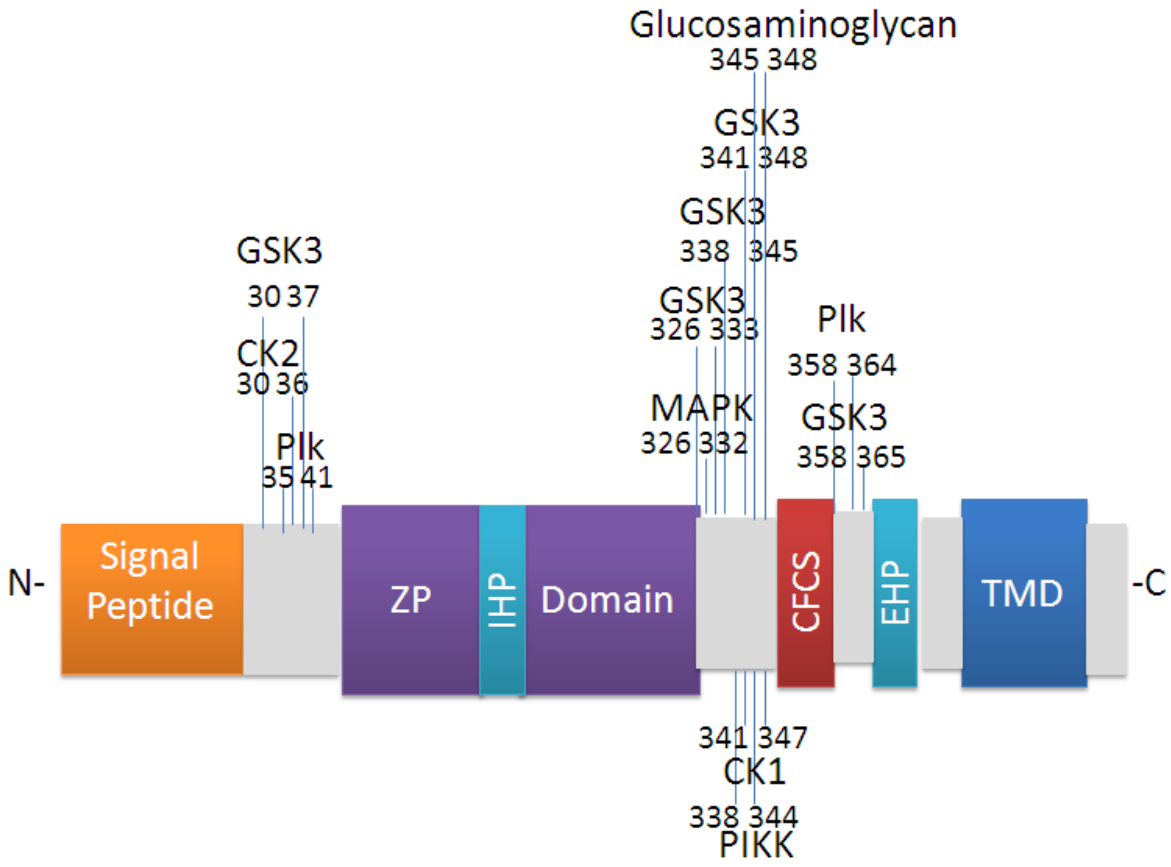

Figure 15. Representation of ZP3 modification sites. CK1, CK2, GSK3, PIKK, Plk and MAPK phosphorylation sites are shown. Glycosaminoglycan attachment site is also shown. CK1, casein kinase 1; CK2, casein kinase 2; GSK3, glycogen synthase kinase 3; PIKK, hosphoinosidite-3-OH-kinase related kinase; Plk, polo-like kinase; MAPK, mitogen-activated kinase.

5.1.5. ZP3 Trafficking

di-Arginine Retention/Retrieval Signal

Di-Arginine-based endoplasmic reticulum (ER)-localization signals are motifs involved in the transport of multimeric proteins and consist of two arginine residues next to each other. These signals can direct a broad range of proteins to the ER and retain them there, but direct mainly membrane protein complexes. In several cases, a di-leucine endocytic or lysosomal targeting signal is also present near di-arginine targeting motifs. Arginine signals can also participate in the regulation of receptor-complex assembly. Contra intuitively, only a minority of proteins with arginine-based signals undergo any modification in the ER. [84].

ELM found one arginine-based signal in ZP3: RNRR (349-352). The software reported the pattern ([LIVMFYWPR]R[^YFWDE] {0,1} R) | (R[^YFWDE] {0,1} R[LIVMFYWPR]) with a probability of approximately 0.005. In this case the pattern has two possible expressions. The first allows leucine, isoleucine, valine, methionine, phenylalanine, tyrosine, tryptophan, proline and arginine in the first position; the second position has an arginine, the third position excludes tyrosine, phenylalanine, tryptophan, aspartate and glutamate or at least one of them, the last position has an arginine. The second condition allowed, has an arginine in the first position, excludes tyrosine, phenylalanine, tryptophan, aspartate and glutamate, or at least one of them; the third position is an arginine and the last allows a leucine, a isoleucine, a valine, a methionine, a phenylalanine, a tyrosine, a tryptophan, a proline and an arginine. The sequence found by ELM in ZP3 is also present in many other proteins, such as human NMDA1, ABCC8, GPR15 and ADAM10.

Endosome-Lysosome-Basolateral Sorting Signals

Several membrane proteins have leucine-based motifs in their cytoplasmic domain to facilitate their internalization. There are two types of motifs, one that is dependent on phosphorylation and another with an acidic amino acid residue which is constitutively active. It was proposed that the position of these motifs within the cytoplasmic domains of receptors may influence their activity at the *trans*-Golgi network and at cell surface [85].

ELM found one endocytic sorting signal in ZP3: QPLWLL (23-28). The pattern [DERQ]...L[LVI] had an approximate probability of 0.003, where the first position has an aspartate, a glutamate, an arginine or a glutamine; the following three positions allow any amino acid, the fifth has leucine and the last allow a leucine, a valine and an isoleucine. The sequence reported by ELM is also present in many other proteins as is the case of human CD4, CD74, CD44 and ATP7A.

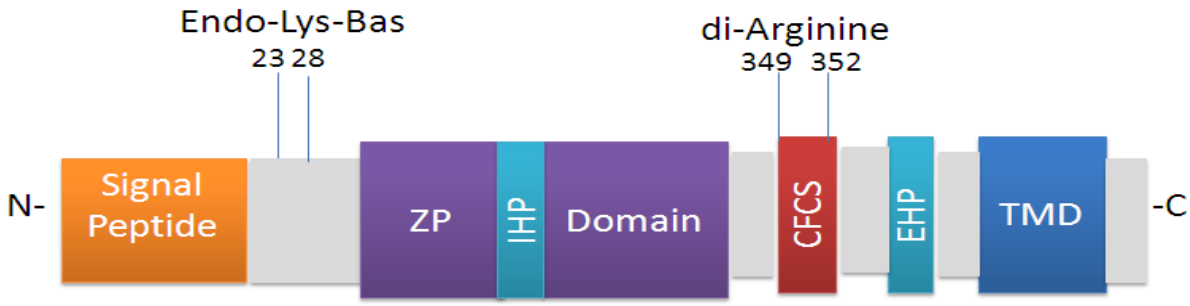

Figure 16. Representation of ZP3 trafficking sites. di-Arginine retention/ retrieval signal and endosome-lysosome-basolateral sorting signal are shown. Endo-Lys-Bas, endosome-lysosome-basolateral sorting signal; di-Arginine, di-Arginine retention/retrieval signal.

5.2. Cell-cell adhesion assays

5.2.1. Procedure optimization

Since this was the first time this procedure was used in the laboratory, it was very important to adequate the experimental conditions to improve results. In a 96-well plate, a feeder layer of 15 000 HeLa cells was plated and incubated overnight at 37ºC in 5% CO_2, in order to be confluent in the following day (approximately 30 000 cells per well). To establish a 'standard adhesion curve', a preliminary test with increasing cell number was performed using HeLa cells, plated on the top of the feeder layer: $1x10^4$, $2x10^4$, $3x10^4$, $5x10^4$, $7{,}5x10^4$ and $10x10^4$ cells. These were incubated for 1h at 37ºC in 5% CO_2, following the protocol in Zepeda-Moreno et al (2011) [65]. Cells that did not adhere in this hour are allowed to fall into the medium by inverting the plate for another 1.5h. These

non-adherent cells were further collected with a micropipette into a new 96-well plate, and resazurin was added to quantify the non-adherent cells. We first tested a final end volume of 330 µL (medium plus resazurin), and incubated this for 4h at 37ºC in 5% CO_2. The experiment was performed in duplicate and culture medium was used as a negative control. After the 4h, the resazurin conversion was spectrophotometrically quantified. This experiment was unsuccessful since all the results were equal to the controls; this could mean that all cells adhered to the feeder layer (more unlikely, or that some technical problems were occurring.

To dismiss that all HeLa cells were actually adhering, we apply the same experimental design, but using the less adherent CHO cell line as the top layer. A feeder layer of HeLa cells was again plated, and CHO cells were added in the following day at increasing cell number (Table 3, line A). CHO cells were also plated directly on the plastic bottom of the 96-well for comparison of the adherence efficiency (Table 3, line B). A row with only culture medium was used as a negative control (Table 3, row 8). After the 1h incubation (adhesion period) and the 1.5h incubation (non-adhesion period), resazurin was added to the 300 µL of the supernatant, and incubated 4h at 37ºC in 5% CO_2.

A photograph of the 96-well plate following the 4h incubation period is shown in Figure 17A. Similarly, there were no differences between the test conditions and controls. To further evaluate whether these results reflected a short incubation period with resazurin, cells were left to incubate with resazurin overnight at 37ºC in 5% CO_2.

Table 3. Scheme of a 96-well plate used in the optimization of the cell-cell adhesion assay, with the number of increasing test cells plated onto the feeder layer, and respective negative controls. Line A: CHO cells plated onto the HeLa feeder layer. Line B: CHO cells plated directly on the plastic bottom of the plate.

	1	2	3	4	5	6	7	8
A	$1x10^4$	$1,5x10^4$	$2x10^4$	$3x10^4$	$4x10^4$	$5,5x10^4$	$7,5x10^4$	Culture Medium
B	$1x10^4$	$1,5x10^4$	$2x10^4$	$3x10^4$	$4x10^4$	$5,5x10^4$	$7,5x10^4$	Culture Medium

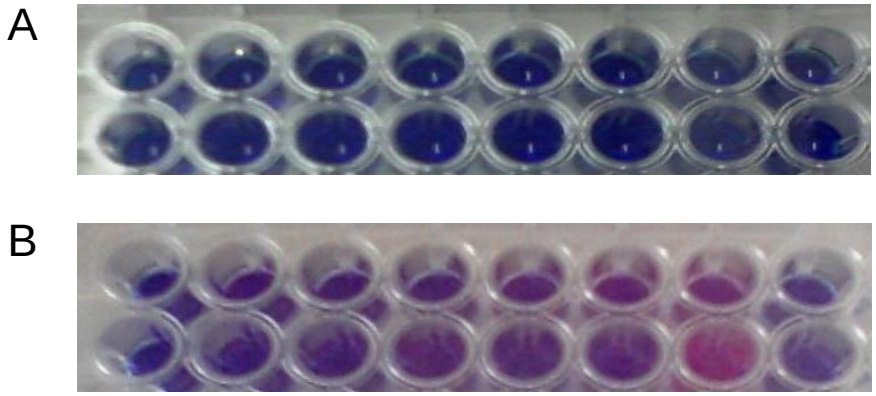

Figure 17. Colorimetric reaction following resazurin incubation. A. Resazurin was metabolized at very low extent after 4h of incubation and all samples were blue/purple. B. After resazurin overnight incubation, cells metabolized resazurin at a higher extent, and the medium colour changed to variations of pink.

After increasing the incubation of cells with resazurin, some cells metabolized resazurin, resulting in a change of colour. A photograph of the 96-well plate following a overnight incubation period is shown in Figure 17B. These results were quantified spectrophotometrically, and are graphically presented in Figure 18.

Low concentrations of non-adherent cells, with slight fluctuations, can be observed for the lowest numbers of plated CHO cells until 30 000 cells, but at 40 000 cells and after there was a linear increase in non-adherent cell concentration (Figure 18A). These results are expected: at lower plated cells number these are still able to adhere to the feeder layer, since the maximum theoretical number of cells per a 96-well plate is of approximately 30 000 (the expected 100% cell confluence). At higher numbers of plated cells it is understandable that there is a decrease in cellular adhesion due to space constriction. After reaching maximum cell confluence, the top cells layer begins to detach from feeder cells, as reflected by the higher cell concentration after 30 000 plated cells (Figure 18A). These results also indicate that this latest experimental design was functional for measuring non-adhesion cells. Of note, a shorter adhesion period of only 30 min was also tested (data not shown) but there were no differences between controls and CHO cells first incubated for 30 minutes, which implies that this is a short incubation period for this experiment.

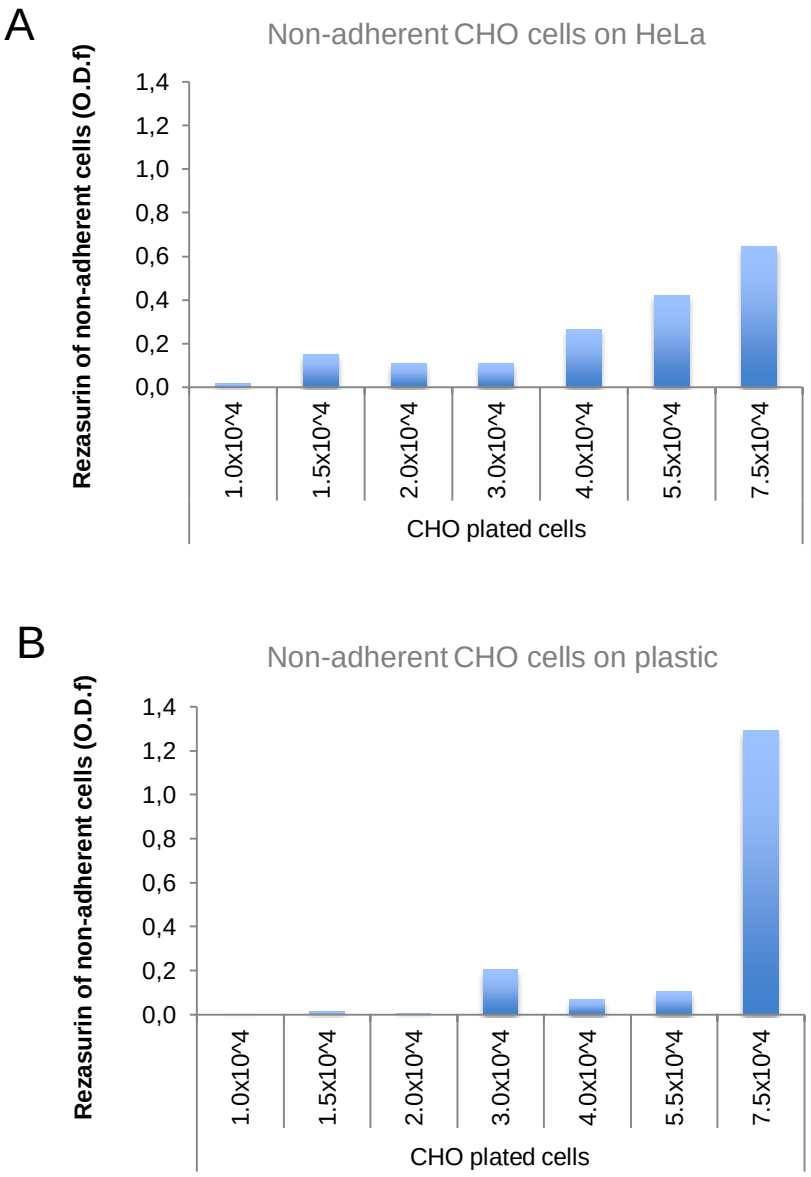

Figure 18. Quantification of non-adherent CHO cells after 1h of adhesion period. **A.** CHO cells plated on a HeLa feeder layer. **B.** CHO cells plated on the plastic bottom. For the increasing number of plated CHO cells, the rate of resazurin conversion is shown, reflecting the non-adherent cells concentration. O.D.f, Final Optic Density.n=2

Figure 18B shows that for the lower-to-medium plated cell number, CHO cells generally adhere better to the plastic than to HeLa cells (10 000 to 55 000 cells). In fact, the number of non-adherent cells was irregular and only at the highest CHO plated number (75 000 cells), the concentration of non-adherent cells was higher in cells incubated on plastic than on HeLa cells (Figure 18B vs 18A).

5.2.2. Characterization of CHO and HeLa Cells Adhesion

CHO-CHO and CHO-plastic Adhesion

The optimized experimental design was then applied to a second set of cell-cell adhesion assays, performed in triplicate, to analyse the adhesion behaviour of CHO and HeLa cells and establish standard curves of non-adherent CHO cells for the following antibody interference assays (section 5.4).

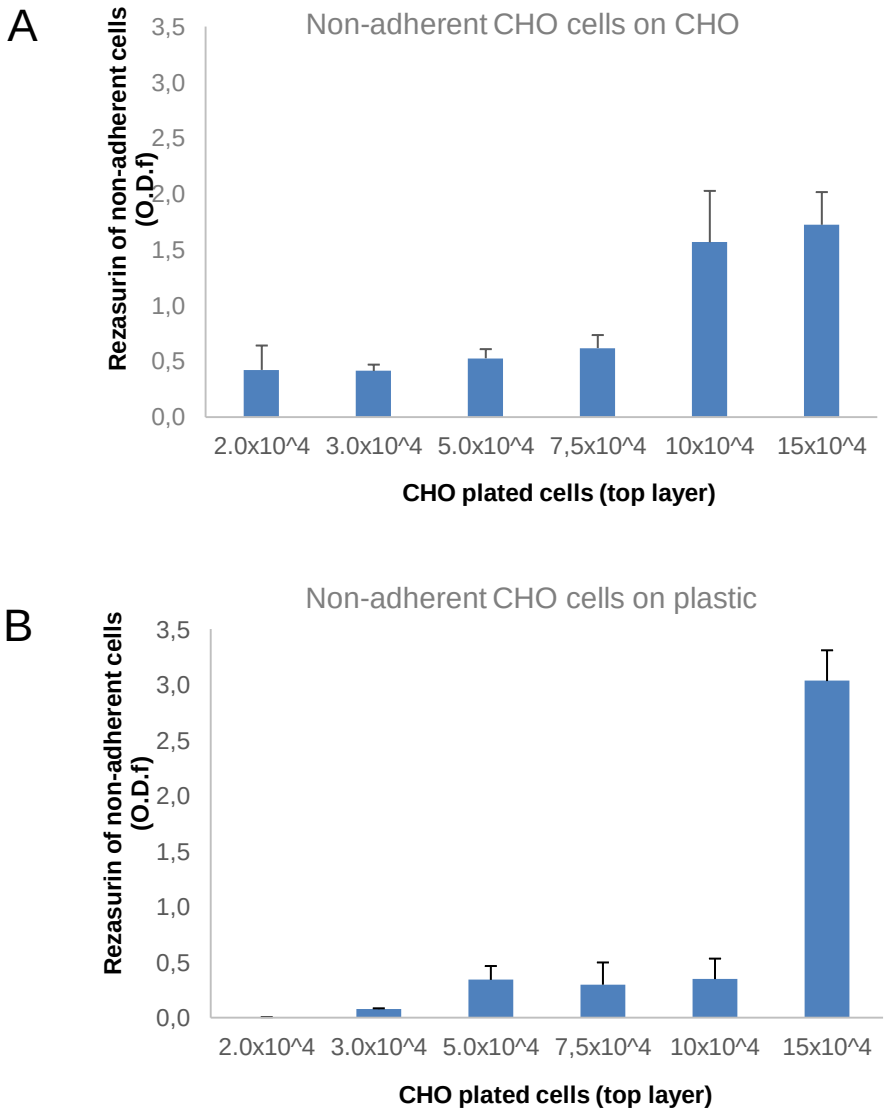

Figure 19. Quantification of non-adherent CHO cells incubated for a 1h adhesion period. **A.** CHO cells plated on a CHO feeder layer. **B.** CHO cells plated directly on the plastic bottom. O.D.f, Final Optic Density. n= 3.

When CHO cells were plated on a CHO feeder layer, again adhesion was greater at lowest than at higher plated cells number (Figure 19A), similar to the previous preliminary results on a HeLa feeder layer (Figure 18A). The first two conditions ($2x10^4$ and $3x10^4$ plated CHO cells) have very similar high adhesion results, and the further two ($5x10^4$ and $7.5x10^4$ cells) present less adhesion (higher concentration of non-adherent cells). A more drastic loss of CHO-CHO cell adhesion occurs only at $10x10^4$ and $15x10^4$ plated CHO cells (Figure 19A). CHO on plastic adhesion results (Figure 19B) are also according to the preliminary ones on Figure 18B: the adhesion of CHO cells to the 96-well plate was very high, again higher than when cells are plated on to a cell feeder layer, since the number of non-adherent cells is quite low. After the 100% confluence, cells start to slightly detach (5-$10x10^4$ plated CHO cells) and only at the highest number tested ($15x10^4$) the concentration of non-adherent cells was very high, but again even higher than for the same number of cells plated on a CHO feeder layer (Figure 19B vs 19A, $15x10^4$ plated cells).

CHO-HeLa Cells Adhesion

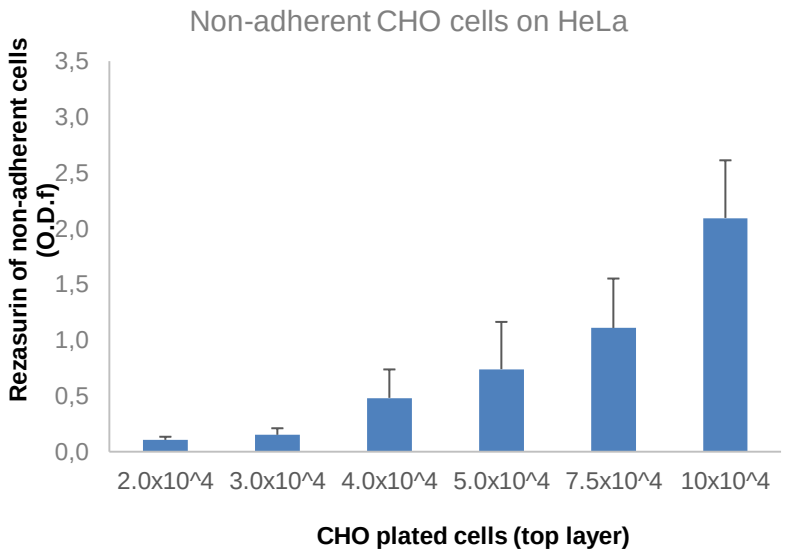

Figure 20. Quantification of non-adherent CHO cells incubated for a 1h adhesion period. on a HeLa feeder layer. O.D.f, Final Optic Density. n= 3.

Similar to the previous CHO-HeLa adhesion assay results (Figure 18A): at the lowest numbers (2 and $3x10^4$ plated cells) almost every cell adhere to the feeder layer. After the confluence threshold of $3x10^4$ cells, CHO cells detach at a linear rate, with the number of non-adherent CHO cells linearly increasing with the number of CHO plated cells (Figure 20).

HeLa-HeLa Cells and HeLa-Plastic Adhesion

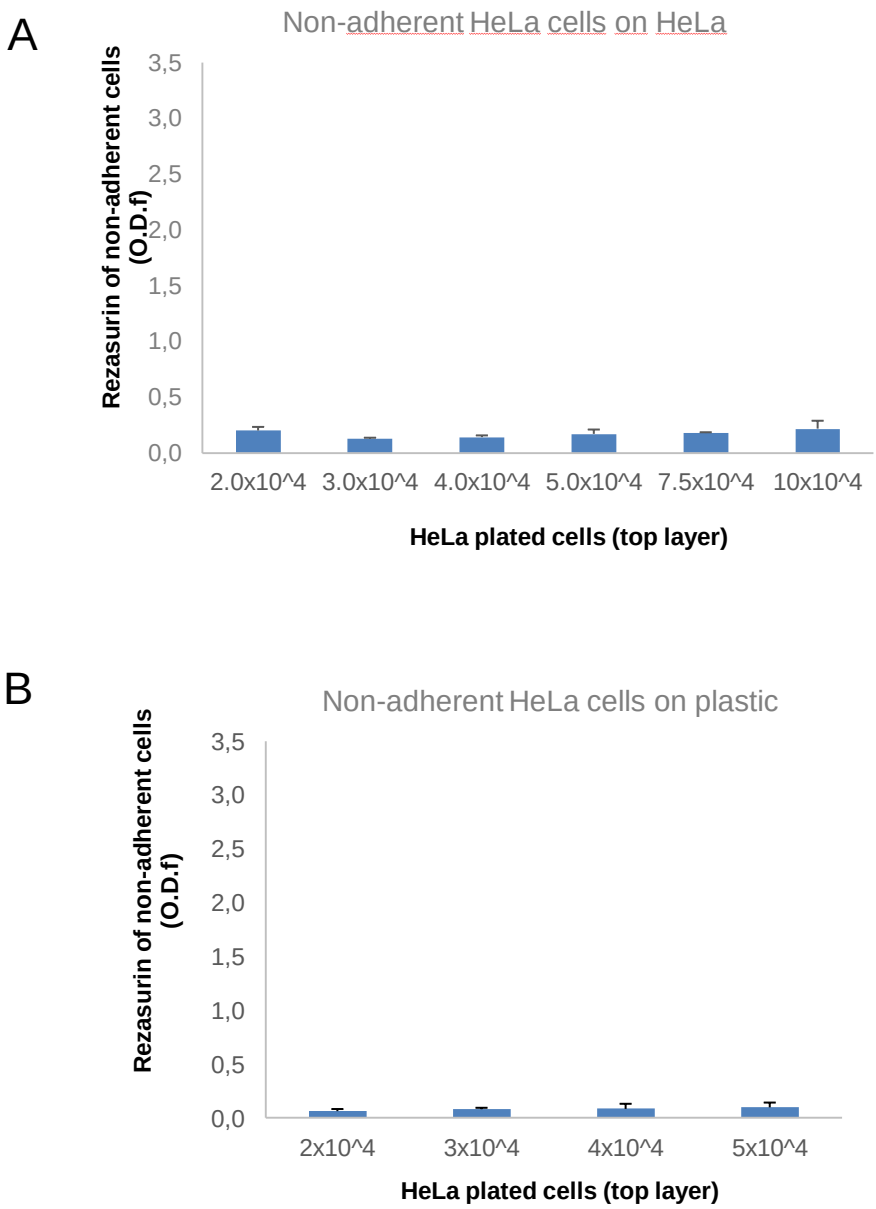

Figure 21. Quantification of non-adherent HeLa cells incubated for a 1h adhesion period. **A.** HeLa cells plated on a HeLa feeder layer. **B.** HeLa cells plated directly on the plastic bottom. O.D.f, Final Optic Density. n= 3.

The adhesive behaviour of the HeLa cells was also studied for comparison reasons (Figure 21). Curiously, almost every HeLa cell adhere to its HeLa feeder layer, even at the highest numbers of plated cells, with only slight variations between all tested plated numbers (Figure 21A). This implies that HeLa cells are able to grow overlapped and strengthens the highly adhesive properties of this cell line, indicating it as a valid choice for a feeder layer in cell-cell adhesion assays, but potentially not very useful as a top layer. Noticeable, the behaviour of HeLa cells adhesion to other HeLa cells or to plastic is very similar (Figure 21B vs 21A), thus reinforcing the adhesive properties of HeLa cells.

5.2.3. Antibody Interference Assays

The same CHO-HeLa cells experimental design was then used in antibody interference assays. A single antibody interference assay was first performed with each of the following antibodies: the 22C11 antibody against the extracellular APP N-terminus, the blocking anti-β1-integrin MAB1959 antibody, and the anti-ZP3 domain antibody. Antibodies dilutions are presented in Table 1.

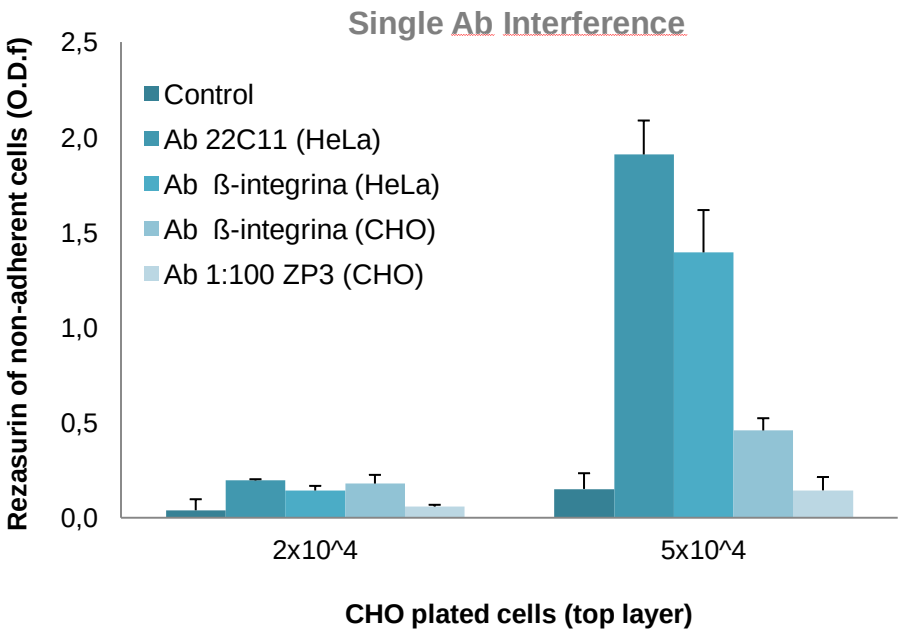

Figure 22. Single antibody interference assay. The HeLa feeder cells or the CHO top cells were pre-incubated with the indicated antibodies before CHO cells plating. Two different CHO cell numbers were tested, pre- and after-confluence. In the control, no antibody was added.

As seen in Figure 22, interfering with APP and β1-integrin, either in HeLa or in CHO cells, increases the loss of CHO cells adhesion at $2x10^4$ CHO plated cells. Interfering with ZP3, by its turn, does not seem to have an effect in cell adhesion. At $5x10^4$ cells, blocking APP and β1-integrin in HeLa cells has a dramatic effect in the loss of CHO cells adhesion. Interfering with β1-integrin in CHO cells also increases the loss of adhesion, although at lower levels than when the antibody is used on HeLa cells. Of note, this reflects the stated much lower sensibility of this antibody to hamster cells (manufacturer's data). Even at a higher CHO cell number, blocking ZP3 appears to have no effect in cell adhesion (Figure 22, '1:100 ZP3'). Of note, a higher concentration of the ZP3 antibody (1:50) was tested (data not shown), but the results were very similar to the ones obtained with the 1:100 dilution.

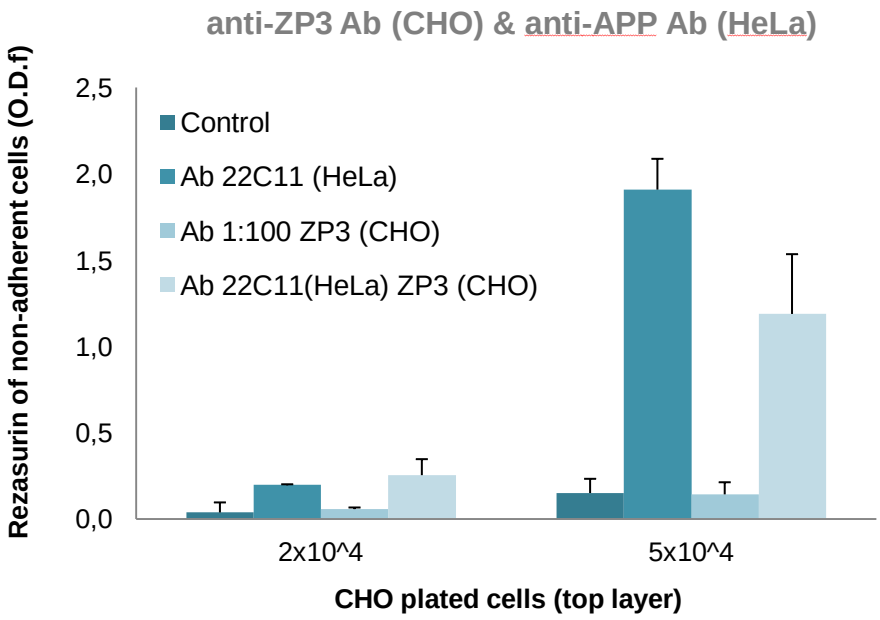

Figure 23. ZP3 and APP co-interference assay. Before CHO cells plating, the HeLa feeder cells were pre-incubated with 22C11 to block APP, and the CHO top cells were pre-incubated with the anti-ZP3 antibody to block ZP3. Two different CHO cell numbers were tested, pre- and after-confluence. In the control, no antibody was added.

When HeLa and CHO cells were simultaneously incubated with the anti-APP and the anti-ZP3 antibodies, at the lowest tested plating cell number, the

effect was similar to the one of APP alone, although a slight increase in the concentration of non-adherent cells (cumulative effect of both antibodies) could be observed, when compared with the single antibodies values (Figure 23, $2x10^4$). At the highest CHO cell number tested, where the anti-APP antibody has a dramatically reducing effect in CHO adhesion, and the anti-ZP3 antibody alone has no effect, the presence of both antibodies appears to slightly decrease the number of non-adherent cells when compared to the 22C11 alone. Hence, blocking ZP3 in addition to APP seems to counteract the effect of blocking APP alone.

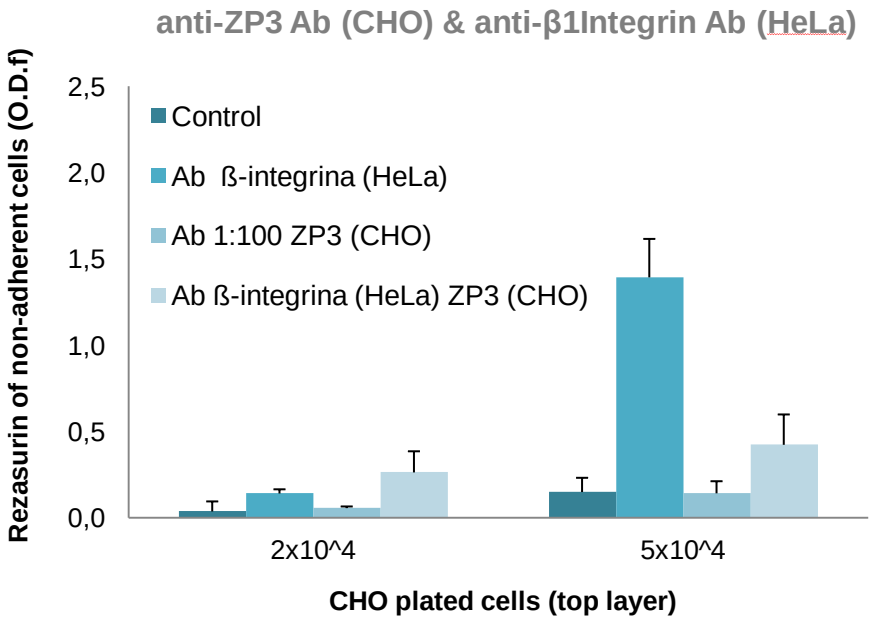

Figure 24. ZP3 and β1-integrin co-interference assay. Before CHO cells plating, the HeLa feeder cells were pre-incubated with MAB1959 to block β1-integrin, and the CHO top cells were pre-incubated with the anti-ZP3 antibody to block ZP3. Two different CHO cell numbers were tested, pre- and after-confluence. In the control, no antibody was added.

Blocking both β1-integrin in HeLa cells and ZP3 in CHO cells, at the $2x10^4$ CHO cells plating number, has a surprising cumulative interference effect in CHO-HeLa cell adhesion (Figure 24). Indeed, there is an increase in the loss of adhesion when compared to each of the effects of the antibodies when alone. This cumulative increase has to be confirmed, as it is still statistically non-significant.

At the highest tested cell number ($5x10^4$), when interfering with β1-integrin alone still has a dramatic effect in the loss of adhesion, and interfering with ZP3 has no observable effect in cell adhesion, blocking both proteins has again the an effect in adhesion, has the number of non-adherent cells increases comparing to controls, however this effect is still lower to that of β1-integrin alone. Similar to what happened in Figure 23 with APP and ZP3, it seems that adding ZP3 decreases the effect of β1-integrin alone (Figure 24, '$5x10^4$').

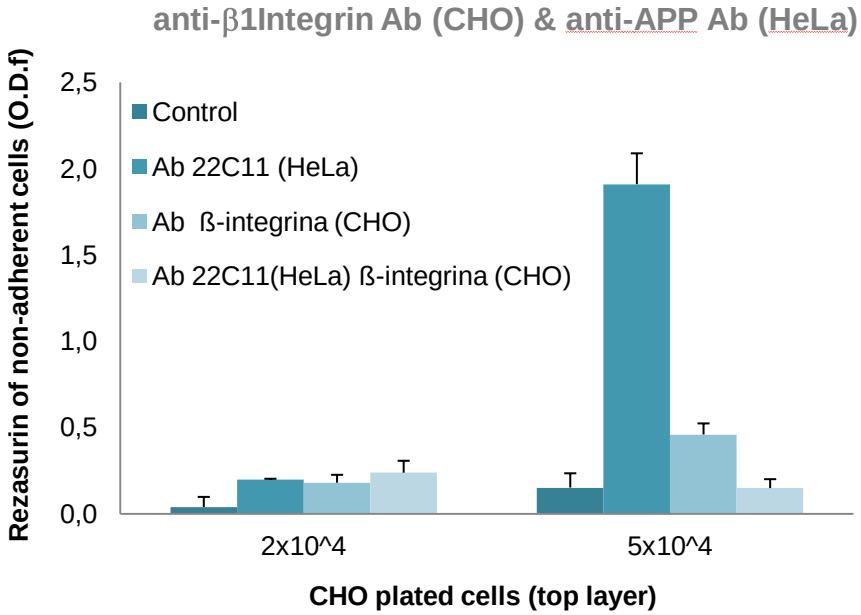

Figure 25. APP and β1-integrin co-interference assay. Before CHO cells plating, the HeLa feeder cells were pre-incubated with 22C11 to block APP, and the CHO top cells were pre-incubated with the MAB1959 to block β1-integrin. Two different CHO cell numbers were tested, pre- and after-confluence. In the control, no antibody was added.

Regarding the effect of simultaneously block APP and β1-integrin, at the subconfluent cell number, when both APP and β1-integrin have single effects in cell adhesion, the blockage of both seems to have a slight cumulative effect (Figure 25, '$2x10^4$'). At the higher CHO cell number, blocking both proteins has again the surprising effect of counteracting the blocking effect of each of the antibodies alone, instead of having the expected cumulative effect observed at $2x10^4$ cells. In fact, there was a dramatic increase in cell adhesion when APP a β1-integrin are simultaneously blocked in each of the cell line (Figure 25, '$5x10^4$').

5.3. Immunocytochemistry assays

In the above antibody interference assays ZP3 appears to somehow influence cell-cell adhesion mediated by APP and β1-integrin. In order to better understand the ZP3 cellular effects, its potential co-localization with APP and β1-integrin was investigated in CHO cells, HeLa cells, and in CHO-HeLa co-cultures.

For analysing ZP3-APP co-localization, the 22C11 antibody was used to detect APP proteins inside cells and in the plasma membrane (Figure 26, red; ZP3 in green). HeLa and CHO have a significant expression of both proteins, being these present throughout the cell in many vesicles, and with APP being specifically abundant in the Golgi apparatus. Of note, ZP3 has also a signal in the cells nuclei, particularly evident for CHO cells, what can be a physiological feature or a mere artefact. Regarding co-localization, there is some co-localization of ZP3 and APP in the Golgi, as expected, since both of them traffic through the secretory pathway. Generally, both ZP3 and APP are absent or present at low amounts at the plasma membrane of both cells, and no or few co-localization between them could be observed in cell-cell contact zones, even in the HeLa:CHO co-culture (Figure 26).

In all the culture conditions tested, the presence of extracellular deposits of secreted ZP3 could be observed (Figure 27). This was especially evident in HeLa cells and in HeLa-CHO co-cultures, since HeLa have apparently higher levels of ZP3. The majority of these extracellular aggregates stained for APP, indicating the presence of this protein in secreted ZP3 oligomers.

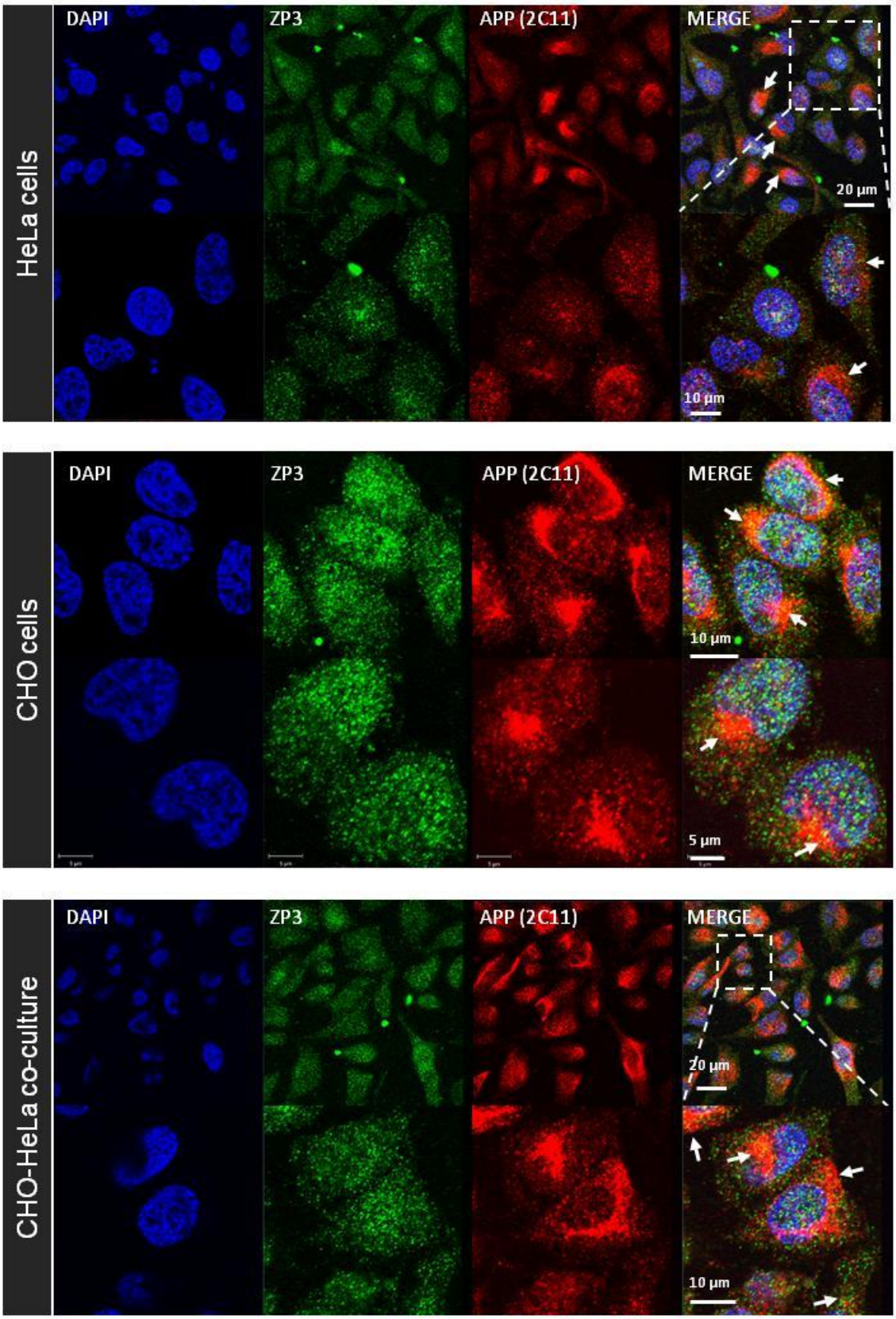

Figure 26. Immunocytochemistry of ZP3 (green fluorescent) and APP (22C11, red fluorescent) in HeLa cells, CHO cells, and in HeLa-CHO co-cultures. Arrows indicate co-localization.

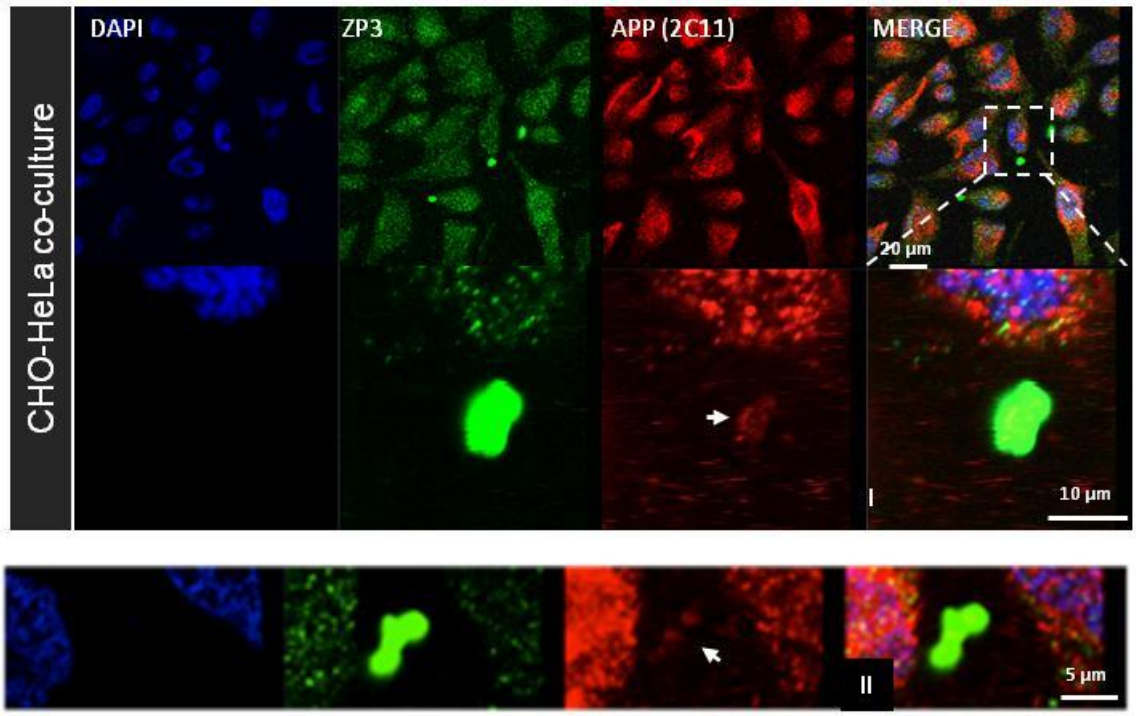

Figure 27. Immunocytochemistry of ZP3 (green fluorescent) and APP (22C11, red fluorescent) in HeLa-CHO co-cultures. I and II indicate different ROIs (regions of interest) zooming in on the ZP3 extracellular aggregates. Arrows indicate the present of APP signal, co-localizing in these structures.

For analysing ZP3-β1-integrin co-localization, the MAB1981 antibody was used to detect the N-terminus of β1-integrin proteins (Figure 28). In HeLa, as previously shown, ZP3 is found inside vesicles, distributed throughout the cell. β1-integrin presents a similar distribution, but is more abundant in cells' nuclei and at the PM than ZP3. There is a higher degree of co-localization between these proteins, when comparing to APP and ZP3. Co-localization is mainly observed in some vesicles, and also near or at the plasma membrane. Comparing to HeLa cells, CHO have a much lower β1-integrin signal, since this antibody does not recognize β1-integrin of hamster origin (data from the manufacturer). The images here presented are overexposed, resulting in a redder image (Figure 28, 'CHO'). The distributions of ZP3 and β1-integrin are similar to the ones in HeLa cells but with lower co-localization. In the co-culture, since the β1-integrin antibody does not detected hamster epitopes, it was used as a marker to distinguish between CHO and HeLa cells. There was not a very high degree of co-localization between both proteins in points of contact between these cells.

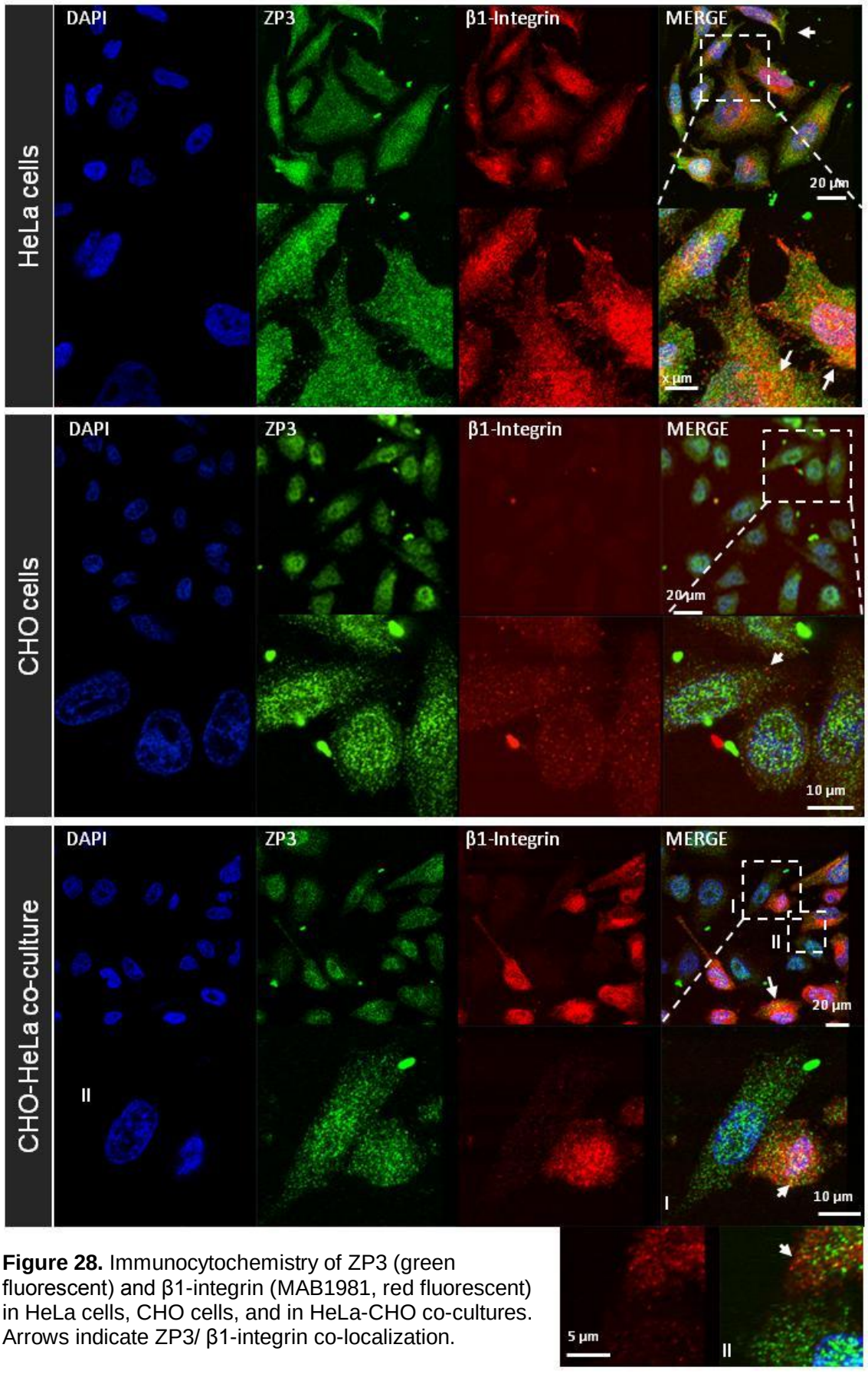

Figure 28. Immunocytochemistry of ZP3 (green fluorescent) and β1-integrin (MAB1981, red fluorescent) in HeLa cells, CHO cells, and in HeLa-CHO co-cultures. Arrows indicate ZP3/ β1-integrin co-localization.

5.4. Immunoprecipitation Assays

To analyse if APP and ZP3 physically interact, as indicated by the extracellular structures where they appear to co-localize (section 5.3), immunoprecipitation assays were performed. First, APP was immunoprecipitated with its CT695 antibody, in duplicate, but using two different magnetic beads linked to protein sepharose G (lane 2 and 3 of the IP).

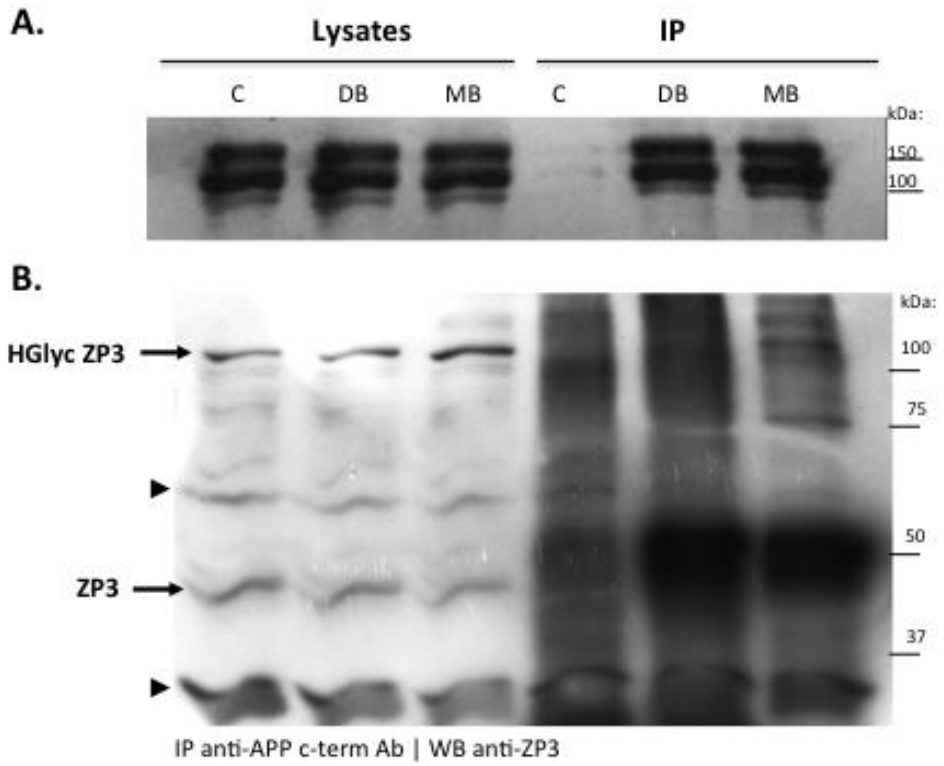

Figure 29. Immunoprecipitation of C-terminus of APP with western blot detection of co-immunoprecipitated ZP3. **A.** WB of APP with the 22C11 antibody. **B.** WB of ZP3. C, control (no primary antibody, only beads). DB, dynabeads (Life Technologies), MB, Millipore beads Arrows indicate different forms of ZP3. HGly, Heavily glycosylated form of ZP3. Arrowheads indicate unspecific bands.

Figure 29A shows that APP was efficiently immunoprecipitated by the CT695 antibody and the magnetic beads. In Figure 29B we can observe that the known 47 kDa ZP3 form could be co-immunoprecipitated with APP, but the dense signal from the immunoglobulins heavy chains around 50 kDa make it difficult to observe. A high glycosylated form of ZP3, slightly above 100 kDa ('HGlyc ZP3'), appeared to be co-immunoprecipitated with APP.

To further clarify and confirm these results, APP and ZP3 were immunoprecipitated, either in the presence or absence of a crosslinker (DSP) to stabilize protein-protein interactions.

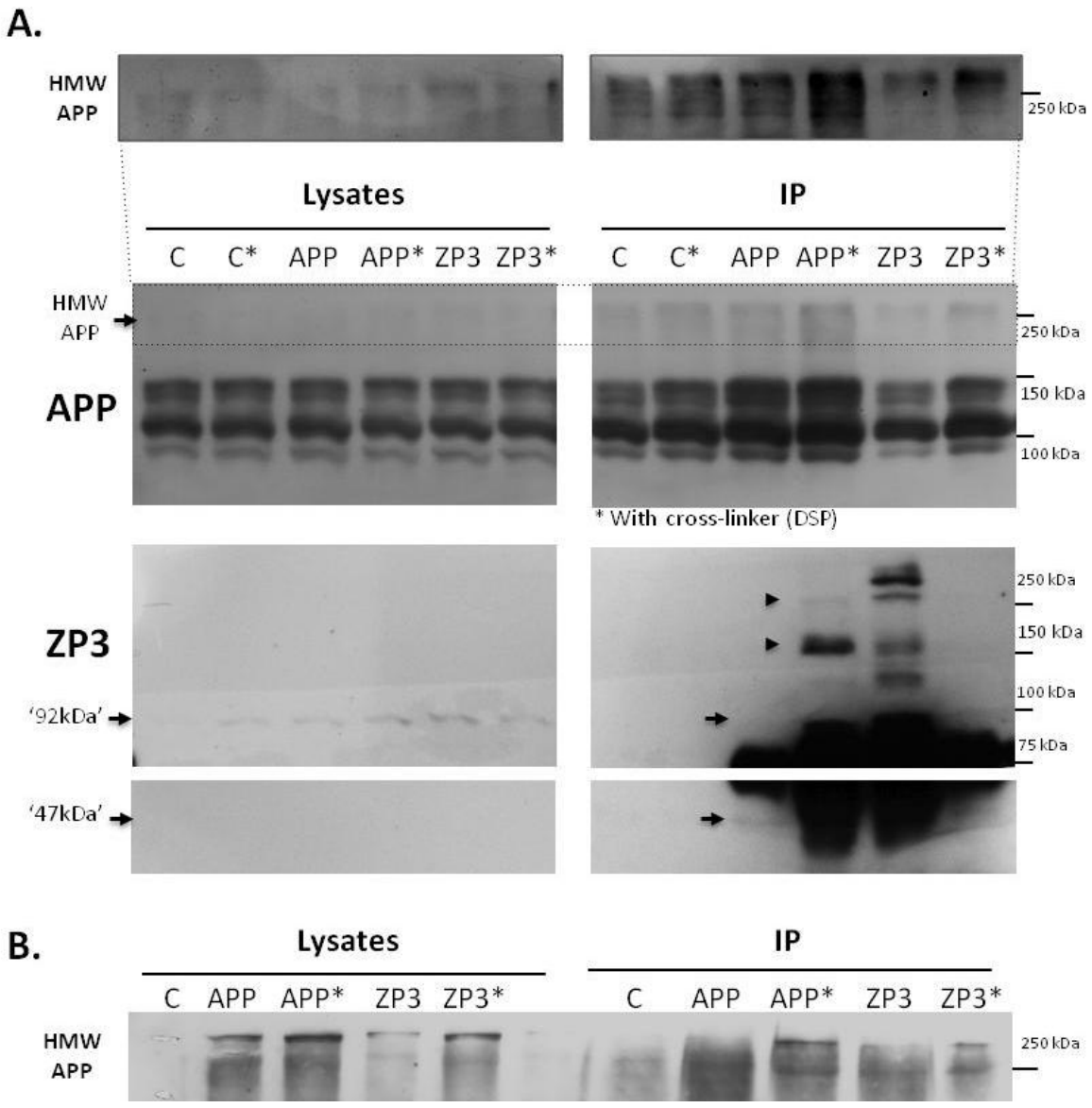

Figure 30. Immunoprecipitation of C-terminus of APP (CT695 Ab) and ZP3 with and without crosslinker. **A.** Western blot was performed for APP (using 22C11) and ZP3. Arrows indicate different known forms of ZP3 of 47 and 92 kDa weights. "92 kDa" and arrowheads indicate heavily glycosylated forms of ZP3. B. Duplicate of experiment A, where highly glycosylated APP co-immunoprecipitated with ZP3 in the presence of the crosslinker.

Unfortunately, the beads here used (Millipore beads) also bound APP in the controls (Figure 30A, ‘C’ in IPs), either in the presence or in the absence of DSP, making it impossible to draw definitive conclusions. Nonetheless, the APP 100-150 kDas forms are more abundant when the CT695 antibody is added (Figure 30A, ‘APP’ in IPs). We can also observe that highly molecular weight (HMW) APP forms are immunoprecipitated more abundantly with the antibodies against APP and ZP3, especially in the presence of the crosslinker (asterisk samples in IPs; highlighted in box). This has been observed in duplicate samples (Figure 30B).

6. Discussion and Conclusions

Cell-cell adhesion is an important step in gamete interactions, and APP and ZP3 are proteins known to be involved in cell-cell adhesion. The distribution of the APP superfamily in the sperm cell, in particular in the sperm head and in the equatorial region [59], indicates a potential role for this protein (and APLPs) in sperm-oocyte adhesion. The ZP glycoprotein ZP3 is currently the main sperm receptor in oocyte-sperm interaction, and thus in this work we intended to understand if APP and ZP3 physically and functionally interact. Since a sperm-oocyte model was not present in the laboratory (although available in the future through collaborations), we started the molecular evaluations by using approximate immortalized cell lines that express ZP3 and APP. The first choice comprehended CHO ovary cells and GC1 spermatogonia cells, but these later did not grow well. HeLa was a second option due to their high levels of APP, ZP3 and other proteins involved in cell-cell adhesion, such as β1-integrin.

A first bioinformatics evaluation of ZP3 revealed some functional motifs that can be of great relevance for APP (section 5.1). For instance, the WW binding motif is also present in the APP binder protein Fe65, also believed to be involved with APP in cell-cell adhesion [63]. Further, both proteins can link high molecular weight carbohydrates such as glucosaminoglycans [60], and ZP3 can be phosphorylated by two kinases up-regulated by APP [82] and our unpublished work). This suggests that there may be a functional relationship between ZP3 and APP.

The adhesion properties of these two glycosylated proteins, APP and ZP3, and their interaction in cell-cell adhesion, were further evaluated (section 5.2). An optimization of a reported cell-cell adhesion procedure was first performed for our cell lines. This method revealed to be very easy to execute, has a low cost, can be performed in a relatively short period of time, and only small amounts of antibodies are needed for the interference assays (section 5.2.1).

When analysing the effects of APP and β1-integrin in cell adhesion, it is noticeable that the blockages of APP and β1-integrin alone (Figure 22) interfered dramatically with CHO-HeLa adhesion, confirming (as expected from the literature) that these two proteins play a crucial role in this process. Noteworthy, these

assays also confirm that the 22C11 can be used as a functional blocking antibody for APP. The addition of the β1-integrin antibody had a surprising biphasic effect on the 22C11-mediated cell detachment (Figure 25). At the lowest tested number (20 000 cells) the influence of both anti-APP and integrin antibodies appear to be slightly cumulative. This suggests that both APP and β1-integrin are involved in the same cell-cell adhesion pathway. However, at the highest number of plated cells (50 000), the cumulative effect is lost and their normal adhesion block, when alone, is completely annulled by the addition of the second blocking antibody (Figure 25).

Blocking ZP3 alone (Figure 22) did not have an effect in disrupting cell adhesion either at the lowest or highest numbers of CHO plated cells, suggesting that it has no or very few adhesive properties by itself, at least for these cells. When both ZP3 and APP proteins were blocked in the interference assays, however, a very slight cumulative effect on disrupting cell adhesion may be observed at the lowest cell number. More interestingly even, when both ZP3 and APP were blocked, again we could observe a decrease in the adhesion disruption first provoked by the anti-APP antibody (Figure 23). Similarly, the simultaneous blockage of ZP3 and β1-integrin had as well this biphasic effect, just like the one seen with APP and ZP3 (Figure 24).

The pre-confluence (20 000 cells) effects here observed are the typical ones observed when studying cell-cell adhesion, and relate to interactions between molecules in the plasma membranes of CHO and HeLa cells, and/or in their secreted extracellular matrices (ECM). The post-confluence (50 000 cells) effects, however, appear to also involve effects mediated by the feeder layer extracellular environment (see section 5.2.1, HeLa-CHO and CHO-CHO adhesion). For example, the alterations provoked by the contact of CHO cells (top layer) with feeder HeLa or CHO cells, turns CHO cells more adhesive at higher cell densities, when compared to the same cells only exposed to plastic (compare Figure 19B with Figure 19A and Figure 20). This has probably to due with the ECM secreted by these feeder layers during the 24h of previous incubation, which influence the adhesive proteome at the cell surface of the CHO top layer.

This does not explain why blocking two adhesive proteins simultaneously at higher cell densities impedes cell detachment. It is possible that, at an overconfluent cell number, there are more APP and β1-integrin molecules at the cell surface left to trans-interact with each other. From the immunocytochemistry assays we observed that APP, ZP3 and β1-integrin co-localize more in the same cell (in potentially cis-interactions) and less in cell-cell contacts. Blocking e.g. β1-integrin in one layer and APP in the other layer may free their habitual cis-APP/ β1-integrin interactors in the same cell, enabling them to CHO-HeLa trans-interact and thus support CHO adhesion.

Overall, these results suggest that the main proteins involved in cell-cell adhesion are APP and β1-integrin, possibly through the same pathway. ZP3 alone seems to have only a slight role in adhesion, but appears to potentiate APP and β1-integrin-mediated cell-cell adhesion, interfering in the APP and β1-integrin pathway.

As described previously, ZP3 and APP traffic through the secretary pathway. Immunocytochemistry assays showed that both proteins co-localized at low extent in the Golgi apparatus in CHO, HeLa and in a co-culture of both cell lines (Figure 26, arrows). A co-localization between these two proteins was further searched in the plasma membrane (PM), however this was very rare. A possible interaction between them at the PM cannot be completely ruled out, since this could be due to the low concentrations of APP and ZP3 in the cell membrane, highlighting that their presence at the PM is highly regulated. Surprisingly, extracellular aggregates of ZP3 were found in all tested cell lines, being particularly abundant in HeLa cells (Figures 26-28). In the great majority of these extracellular ZP3 aggregates we could observe some degree of co-localization with APP (Figure 27), and even with β1-integrin (Figure 28). This suggests that APP may interact with ZP3 dimers when they are both secreted into the ECM.

The MAB1981 antibody we have used is almost non-functional in hamster samples. This is readily visible in the CHO cells cultures of Figure 28, which have a very low β1-integrin signal (red fluorescence). Therefore, in a co-culture of HeLa and CHO cells, ZP3 and β1-integrin have functioned as cell markers, facilitating the distinction between both cell lines (Figure 28, ‘co-culture’). We were not able to

observe considerable co-localization between these two proteins in different cells in contact. Contrary, in HeLa cells, ZP3 and β1-integrin co-localize with a higher degree than ZP3 and APP, especially at the plasma membrane (Figure 28). This is in accordance with their higher synergistic effect observed in the interference assays (Figure 24).

From the immunoprecipitation assays it remained unclear whether APP and ZP3 physically interact (Figures 29 and 30). Although inconclusive, a possible interaction between ZP3 and APP potentially exists, in particular in between their highly glycosylated forms. This would be in line with the immunocytochemistry findings of their co-localization in aggregates of the ECM, but more experiments are needed to prove that these proteins physically interact and understand their relationship in cell-cell adhesion. This would be of particular interest in sperm-oocyte interaction, where protein-carbohydrate interactions are accepted to be highly important [3], [12], [29]–[31], and glycosylation is crucial for triggering the acrosome reaction [29]–[31].

Also importantly, in this work we cannot dismiss overlapping functions between APP and APLP2, with whom APP shares a high homology at its N-terminus, and that is also recognized by the 22C11 antibody.

Conclusions

This work allowed the introduction of a novel cell-cell adhesion procedure in the laboratory that can be easily performed and is already optimized for each of the tested cell lines (HeLa and CHO).

Regarding cell-cell adhesion, of all the studies proteins: APP, β1-integrin and ZP3, the first two appear to play a more crucial role in this process, possibly through a common pathway, while ZP3 appears to play a secondary role. ZP3 slight effect in cell adhesion is potentially via interaction with APP and β1-integrin since it interferes with the effect of those proteins in cellular adhesion similarly as they do with each other.

Intracellular ZP3 only co-localized at low amounts with APP, and in organelles involved in their secretory pathway. However, it showed a higher

degree of co-localization with β1-integrin in vesicles and at the plasma membrane. Unexpectedly, the presence of extracellular aggregates of ZP3, most of which contained small amounts of APP was observed. Some of those deposits appear to also have β1-integrin signal, potentially indicating that these aggregates form in ECM locations where β1-integrin exists.

7. References

[1] P. Talbot, B. D. Shur, and D. G. Myles, “Cell Adhesion and Fertilization: Steps in Oocyte Transport, Sperm-Zona Pellucida Interactions, and Sperm-Egg Fusion,” *Biol. Reprod.*, vol. 68, pp. 1–9, Oct. 2003.

[2] S. K. Gupta, P. Bansal, A. Ganguly, B. Bhandari, and K. Chakrabarti, “Human zona pellucida glycoproteins: functional relevance during fertilization,” *J. Reprod. Immunol.*, vol. 83, pp. 50–55, 2009.

[3] S. K. Gupta, B. Bhandari, A. Shrestha, and B. K. Biswal, “Mammalian zona pellucida glycoproteins: structure and function during fertilization,” *Cell Tissue Res*, pp. 665–678, 2012.

[4] F. Sinowatz, E. Toèpfer-Petersen, S. Koèlle, and G. Palma, “Functional Morphology of the Zona Pellucida,” *Anat. Histol. Embryol*, vol. 263, no. 30, pp. 257–2663, 2001.

[5] H. Okumura, N. Aoki, C. Sato, D. Nadano, and T. Matsuda, “Heterocomplex Formation and Cell-Surface Accumulation of Hen ’ s Serum Zona Pellucida B1 (ZPB1) with ZPC Expressed by a Mammalian Cell Line (COS-7): A Possible Initiating Step of Egg-Envelope Matrix Construction,” *Biol. Reprod.*, vol. 18, no. 76, pp. 9–18, 2007.

[6] A. T. Reid, K. Redgrove, R. J. Aitken, and B. Nixon, “Cellular mechanisms regulating sperm – zona pellucida interaction,” *Asian J. Androl.*, no. 13, pp. 88–96, 2011.

[7] P. M. Wassarman and E. S. Litscher, “Mammalian fertilization: the egg’s multifunctional zona pellucida.,” *Int. J. Dev. Biol.*, vol. 52, no. 5–6, pp. 665–76, Jan. 2008.

[8] P. M. Wassarman, L. Jovine, E. S. Litscher, H. Qi, and Z. Williams, “Egg – sperm interactions at fertilization in mammals,” *Eur. J. Obstet. Gynecol. Reprod. Biol.*, no. 115, pp. 57–60, 2004.

[9] P. M. Wassarman, “Zona Pellucida Glycoproteins,” *Ann. Rev. Biochem*, no. 57, pp. 415–442, 1988.

[10] P. Nandi, S. Ghosh, K. Jana, and P. C. Sen, “Elucidation of the involvement of p14, a sperm protein during maturation, capacitation and acrosome reaction of caprine spermatozoa.,” *PLoS One*, vol. 7, no. 1, p. e30552, Jan. 2012.

[11] M. Jiménez-Movilla, M. Avile, P. Jose, T. Castells, J. De Juan, and A. Romeu, “Carbohydrate analysis of the zona pellucida and cortical granules of human oocytes by means of ultrastructural cytochemistry,” *Hum. Reprod.*, vol. 19, no. 8, pp. 1842–1855, 2004.

[12] S. Chakravarty, S. Kadunganattil, P. Bansal, R. K. Sharma, and S. K. Gupta, “Relevance of Glycosylation of Human Zona Pellucida Glycoproteins for Their Binding to Capacitated Human Spermatozoa and Subsequent Induction of Acrosomal Exocytosis,” *Mol. Reprod. Dev.*, vol. 88, no. 75, pp. 75–88, 2008.

[13] T. Rankin and J. Dean, “The zona pellucida: using molecular genetics to study the mammalian egg coat.,” *Rev. Reprod.*, vol. 5, no. 2, pp. 114–21, May 2000.

[14] G. Goudet, S. Mugnier, I. Callebaut, and P. Monget, “Phylogenetic Analysis and Identification of Pseudogenes Reveal a Progressive Loss of Zona Pellucida Genes During Evolution of Vertebrates,” *Biol. Reprod.*, vol. 806, no. 78, pp. 796–806, 2008.

[15] P. M. Wassarman and E. S. Litscher, “The multifunctional zona pellucida and mammalian fertilization.,” *J. Reprod. Immunol.*, vol. 83, pp. 45–9, Dec. 2009.

[16] W. J. Swanson, Z. Yang, M. F. Wolfner, and C. F. Aquadro, “Positive Darwinian selection drives the evolution of several female reproductive proteins in mammals,” *PNAS*, vol. 98, no. 5, pp. 2509–2514, 2001.

[17] K. G. Claw and W. J. Swanson, “Evolution of the egg: new findings and challenges.,” *Annu. Rev. Genomics Hum.*, vol. 13, pp. 109–25, Jan. 2012.

[18] N. N. Louros, V. a Iconomidou, P. Giannelou, and S. J. Hamodrakas, “Structural analysis of peptide-analogues of human Zona Pellucida ZP1 protein with amyloidogenic properties: insights into mammalian Zona Pellucida formation.,” *PLoS One*, vol. 8, no. 9, p. e73258, Jan. 2013.

[19] L. Jovine and M. Monné, “A Structural View of Egg Coat Architecture and Function in Fertilization,” *Biol. Reprod.*, vol. 669, no. 85, pp. 661–669, 2011.

[20] L. Jovine, H. Qi, Z. Williams, E. S. Litscher, and P. M. Wassarman, “A duplicated motif controls assembly of zona pellucida domain proteins,” *PNAS*, vol. 101, no. 16, pp. 5922–5927, 2004.

[21] B. S. Dunbar, S. Avery, V. Lee, S. Prasad, D. Schwahn, E. Schwoebel, S. Skinner, and B. Wilkins, “The Mammalian Zona Pellucida□: its Biochemistry , Immunochemistry , Molecular Biology , and Developmental Expression,” *Reprod. Fertil. Dev.*, vol. 6, pp. 331–347, 1994.

[22] P. C. N. Chiu, B. S. T. Wong, C. L. Lee, R. T. K. Pang, K. Lee, S. B. Sumitro, S. K. Gupta, and W. S. B. Yeung, “Native human zona pellucida glycoproteins□: purification and binding properties,” *Hum. Reprod.*, vol. 23, no. 6, pp. 1385–1393, 2008.

[23] A. R. Bauskin, D. R. Franken, U. Eberspaecher, and P. Donner, “Characterization of human zona pellucida glycoproteins,” *Mol. Hum. Reprod.*, vol. 5, no. 6, pp. 534–540, 1999.

[24] S. K. Gupta and B. Bhandari, “Acrosome reaction: relevance of zona pellucida glycoproteins.,” *Asian J. Androl.*, vol. 13, no. 1, pp. 97–105, Jan. 2011.

[25] D. P. L. Green, “Three-dimensional structure of the zona pellucida,” *Rev. Reprod.*, vol. 2, pp. 147–156, 1997.

[26] A. D. Burkart, B. Xiong, B. Baibakov, M. Jiménez-Movilla, and J. Dean, “Ovastacin, a cortical granule protease, cleaves ZP2 in the zona pellucida to prevent polyspermy.,” *J. Cell Biol.*, vol. 197, no. 1, pp. 37–44, Apr. 2012.

[27] H. Tsubamoto, A. Hasegawa, Y. Nakata, S. Naito, N. Yamasaki, and K. Koyama, “Expression of Recombinant Human Zona Pellucida Protein 2 and Its Binding Capacity to Spermatozoa,” *Biol. Reprod.*, no. 61, pp. 1649–1654, 1999.

[28] M. E. Chamberlin and J. Dean, “Human homolog of the mouse sperm receptor.,” *Proc. Nat. Acad. Sci. USA*, vol. 87, no. 16, pp. 6014–8, Aug. 1990.

[29] P. Bansal, K. Chakrabarti, and S. K. Gupta, “Functional Activity of Human ZP3 Primary Sperm Receptor Resides Toward Its C-Terminus,” *Biol. Reprod.*, vol. 81, pp. 7–15, 2009.

[30] P. C. N. Chiu, B. S. T. Wong, M.-K. Chung, K. K. W. Lam, R. T. K. Pang, K.-F. Lee, S. B. Sumitro, S. K. Gupta, and W. S. B. Yeung, “Effects of native human zona pellucida glycoproteins 3 and 4 on acrosome reaction and zona pellucida binding of human spermatozoa.,” *Biol. Reprod.*, vol. 79, no. 5, pp. 869–77, Nov. 2008.

[31] P. Caballero-Campo, M. Chirinos, X. J. Fan, M. E. González-González, M. Galicia-Chavarría, F. Larrea, and G. L. Gerton, “Biological effects of recombinant human zona pellucida proteins on sperm function.,” *Biol. Reprod.*, vol. 74, no. 4, pp. 760–8, Apr. 2006.

[32] D. Y. Liu, M. L. Liu, G. N. Clarke, and H. W. G. Baker, “Hyperactivation of capacitated human sperm correlates with the zona pellucida-induced acrosome reaction of zona pellucida-bound sper,” *Hum. Reprod.*, vol. 22, no. 10, pp. 2632–2638, 2007.

[33] B. Baibakov, L. Gauthier, P. Talbot, T. L. Rankin, and J. Dean, “Sperm binding to the zona pellucida is not sufficient to induce acrosome exocytosis.,” *Development*, vol. 134, no. 5, pp. 933–43, Mar. 2007.

[34] A. Ganguly, P. Bansal, T. Gupta, and S. K. Gupta, "' ZP domain ' of human zona pellucida glycoprotein-1 binds to human spermatozoa and induces acrosomal exocytosis," pp. 11–14, 2010.

[35] L. Jovine, C. C. Darie, E. S. Litscher, and P. M. Wassarman, "Zona Pellucida Domain Proteins," *Annu. Rev. Biochem*, no. 74, pp. 83–114, 2005.

[36] M. Zhao, L. Gold, H. Dorward, L. Liang, T. Hoodbhoy, E. S. Boja, H. M. Fales, and J. Dean, "Mutation of a Conserved Hydrophobic Patch Prevents Incorporation of ZP3 into the Zona Pellucida Surrounding Mouse Eggs," *Mol. Cell. Biol.*, vol. 23, no. 24, pp. 8982–8991, 2003.

[37] S. M. Kiefer, P. Saling, and N. Carolina, "Proteolytic Processing of Human Zona Pellucida Proteins," *Biol. Reprod.*, vol. 414, no. 66, pp. 407–414, 2002.

[38] L. Jovine, H. Qi, Z. Williams, E. Litscher, and P. M. Wassarman, "The ZP domain is a conserved module for polymerization of extracellular proteins," *Nat. Cell Biol.*, vol. 4, pp. 457–461, 2002.

[39] S. Santambrogio, S. Perucca, G. Casari, and L. Rampoldi, "Analysis of Uromodulin Polymerization Provides New Insights into the Mechanisms Regulating ZP Domain-mediated Protein Assembly," *Mol. Biol. Cell*, vol. 20, pp. 589–599, 2009.

[40] M. Jiménez-Movilla and J. Dean, "ZP2 and ZP3 Cytoplasmic Tails Prevent Premature Interactions and Ensure Incorporation Into The Zona Pellucida," *J Cell Sci*, vol. 124, no. 6, pp. 940–950, 2011.

[41] B. D. Shur, "Reassesing the role of protein-carbohydrate complementarity during sperm-egg interactions in the mouse," *Int. J. Dev. Biol.*, vol. 52, no. 5–6, pp. 703–715, 2008.

[42] B. Nixon, R. J. Aitken, and E. A. McLaughlin, "New insights into the molecular mechanisms of sperm-egg interaction," *Cell. Mol. Life Sci.*, vol. 64, pp. 1805–1823, 2007.

[43] U. Vjugina and J. P. Evans, "New insights into the molecular basis of mammalian sperm-egg interactions," *Front. Biosci*, vol. 13, pp. 462–476, 2008.

[44] Y. Takahashi, D. Bigler, Y. Ito, and J. M. White, "Sequence-specific interaction between the disintegrin domain of mouse ADAM 3 and murine eggs: role of beta1 integrin-associated proteins CD9, CD81, and CD98.," *Mol. Biol. Cell*, vol. 12, no. 4, pp. 809–20, Apr. 2001.

[45] A. Ashrafzadeh, S. A. Karsani, and S. Nathan, "Mammalian sperm fertility related proteins.," *Int. J. Med. Sci*, vol. 10, no. 12, pp. 1649–57, Jan. 2013.

[46] U. V Desiderio, X. Zhu, and J. P. Evans, “ADAM2 interactions with mouse eggs and cell lines expressing α4/α9 (ITGA4/ITGA9) integrins: implications for integrin-based adhesion and fertilization.,” *PLoS One*, vol. 5, no. 10, p. e13744, Jan. 2010.

[47] S. Tardif and N. Cormier, “Role of zonadhesin during sperm – egg interaction : a species-specific acrosomal molecule with multiple functions,” *Mol. Hum. Reprod.*, vol. 17, no. 11, pp. 661–668, 2011.

[48] N. Inoue, M. Ikawa, and M. Okabe, “The mechanism of sperm-egg interaction and the involvement of IZUMO1 in fusion.,” *Asian J. Androl.*, vol. 13, no. 1, pp. 81–7, Jan. 2011.

[49] A. Ziyyat, E. Rubinstein, F. Monier-gavelle, V. Barraud, O. Kulski, M. Prenant, C. Boucheix, M. Bomsel, and J. Wolf, “CD9 controls the formation of clusters that contain tetraspanins and the integrin alpha 6 beta 1 , which are involved in human and mouse gamete fusion,” *J. Cell Sci.*, vol. 151, pp. 416–424, 2006.

[50] D. Chan, C. J. Thomas, V. J. Taylor, and R. D. Burke, “Integrins on eggs: focal adhesion kinase is activated at fertilization, forms a complex with integrins, and is necessary for cortex formation and cell cycle initiation.,” *Mol. Biol. Cell*, vol. 24, no. 21, pp. 3472–81, Nov. 2013.

[51] C. Tatone and M. C. Carbone, “Possible involvement of integrin-mediated signalling in oocyte activation: evidence that a cyclic RGD-containing peptide can stimulate protein kinase C and cortical granule exocytosis in mouse oocytes.,” *Reprod. Biol. Endocrinol.*, vol. 4, p. 48, Jan. 2006.

[52] K. A. Baessler, Y. Lee, and N. S. Sampson, “β1 Integrin is an Adhesion Protein for Sperm Binding to Eggs,” *ACS Chem Biol.*, vol. 4, no. 5, pp. 357–366, 2010.

[53] P. M. Wassarman, L. Jovine, H. Qi, Z. Williams, C. Darie, and E. S. Litscher, “Recent aspects of mammalian fertilization research,” *Mol. Cell. Endocrinol.*, vol. 234, pp. 95–103, 2005.

[54] L. J. Vella and R. Cappai, “Identification of a novel amyloid precursor protein processing pathway that generates secreted N-terminal fragments,” *FASEB J.*, vol. 26, pp. 2930–2940, 2012.

[55] S. S. A. An and S. Kim, “The genetics of Alzheimer ’ s disease,” *Clin. Interv. Aging*, vol. 9, pp. 535–551, 2014.

[56] R. Sandbrink, C. L. Mastersn, and K. Beyreuthers, “βA4-Amyloid Protein Precursor mRNA Isoforms without Exon 15 Are Ubiquitously Expressed in Rat Tissues Including Brain , but Not in Neurons *,” *J. Biol. Chem.*, vol. 269, no. 2, pp. 1510–1517, 1994.

[57] F. Baumkötter, K. Wagner, S. Eggert, K. Wild, and S. Kins, “Structural aspects and physiological consequences of APP/APLP trans-dimerization.,” *Exp. Brain Res.*, vol. 217, pp. 389–95, Apr. 2012.

[58] R. Sandbrink, C. L. Masters, and K. Beyreutherb, “APP Gene Family: Alternative Slicing Generates Functionally Related Isoforms,” *Ann. New York Acad. Sci.*, vol. 777, pp. 281–287, 1996.

[59] M. Fardilha, S. I. Vieira, and A. Barros, “Differential Distribution of Alzheimer ’ s Amyloid Precursor Protein Family Variants in Human Sperm,” *Ann. New York Acad. Sci.*, vol. 1096, pp. 196–206, 2007.

[60] M. N. Pangalos, S. Efthimiopoulos, J. Shioi, and N. K. Robakis, “The Chondroitin Sulfate Attachment Site of Appican Is Formed by Splicing Out Exon 15 of the Amyloid Precursor Gene,” *J. Biol. Chem.*, vol. 270, no. 18, pp. 10388–10391, May 1995.

[61] P. Soba, S. Eggert, H. Zentgraf, S. Kreger, A. Lo, A. Langer, G. Merdes, C. L. Masters, U. Mu, S. Kins, and K. Beyreuther, “Homo- and heterodimerization of APP family members promotes intercellular adhesion,” *EMBO J.*, vol. 24, pp. 3624–3634, 2005.

[62] M. Asada-Utsugi, K. Uemura, Y. Yoda, and A. Kuzuya, “N-cadherin enhances APP dimerization at the extracellular domain and modulates Aβ production,” *J Neurochem*, vol. 119, no. 2, pp. 354–363, 2011.

[63] S. L. Sabo, a F. Ikin, J. D. Buxbaum, and P. Greengard, “The Alzheimer amyloid precursor protein (APP) and FE65, an APP-binding protein, regulate cell movement.,” *J. Cell Biol.*, vol. 153, no. 7, pp. 1403–14, Jun. 2001.

[64] T. L. Young-Pearse, A. C. Chen, R. Chang, C. Marquez, and D. J. Selkoe, “Secreted APP regulates the function of full-length APP in neurite outgrowth through interaction with integrin beta1.,” *Neural Dev.*, vol. 3, no. June, p. 15, Jan. 2008.

[65] A. Zepeda-Moreno, I. Taubert, I. Hellwig, V. Hoang, L. Pietsch, V. K. Lakshmanan, W. Wagner, and A. D. Ho, “Innovative method for quantification of cell-cell adhesion in 96-well plates,” *Cell Adh. Migr.*, vol. 5, no. 3, pp. 215–219, May 2011.

[66] V. Hospital, V. Chesneau, A. Balogh, C. Joulie, N. G. Seidah, P. Cohen, and A. Prat, “N-arginine dibasic convertase (nardilysin) isoforms are soluble dibasic-specific metalloendopeptidases that localize in the cytoplasm and at the cell surface.,” *Biochem. J.*, vol. 349, no. Pt 2, pp. 587–97, Jul. 2000.

[67] A. R. Pierotti, A. Prat, V. Chesneau, F. Gaudoux, A. Leseney, T. Foulon, P. Cohent, L. De Biochimie, R. Cellulaires, U. Pierre, U. De Recherches, N. De, R. Scientifique, and B. Raspail, “N-Arginine dibasic convertase, a

metalloendopeptidase as a prototype of a class of processing enzymes," *Biochemistry*, vol. 91, pp. 6078–6082, 1994.

[68] S. S. Molloy, P. a Bresnahan, S. H. Leppla, K. R. Klimpel, and G. Thomas, "Human furin is a calcium-dependent serine endoprotease that recognizes the sequence Arg-X-X-Arg and efficiently cleaves anthrax toxin protective antigen.," *J. Biol. Chem.*, vol. 267, no. 23, pp. 16396–402, Aug. 1992.

[69] N. G. Seidah, S. J. Mowla, J. Hamelin, a M. Mamarbachi, S. Benjannet, B. B. Touré, A. Basak, J. S. Munzer, J. Marcinkiewicz, M. Zhong, J. C. Barale, C. Lazure, R. a Murphy, M. Chrétien, and M. Marcinkiewicz, "Mammalian subtilisin/kexin isozyme SKI-1: A widely expressed proprotein convertase with a unique cleavage specificity and cellular localization.," *Proc. Natl. Acad. Sci. U. S. A.*, vol. 96, pp. 1321–6, Feb. 1999.

[70] A. D. Olmstead, W. Knecht, I. Lazarov, S. B. Dixit, and F. Jean, "Human subtilase SKI-1/S1P is a master regulator of the HCV Lifecycle and a potential host cell target for developing indirect-acting antiviral agents.," *PLoS Pathog.*, vol. 8, no. 1, p. e1002468, Jan. 2012.

[71] M. N. Holowaty, Y. Sheng, T. Nguyen, C. Arrowsmith, and L. Frappier, "Protein interaction domains of the ubiquitin-specific protease, USP7/HAUSP.," *J. Biol. Chem.*, vol. 278, no. 48, pp. 47753–61, Nov. 2003.

[72] P. Lu, X. Z. Zhou, M. Shen, and K. Lu, "Function of WW Domains as Phosphoserine- or Phosphothreonine-Binding Modules," *Science (80-.).*, vol. 283, no. 5406, pp. 1325–1328, Feb. 1999.

[73] M. Sudol, K. Sliwa, and T. Russo, "Functions of WW domains in the nucleus.," *FEBS Lett.*, vol. 490, no. 3, pp. 190–5, Feb. 2001.

[74] J. R. Bradley and J. S. Pober, "Tumor necrosis factor receptor-associated factors (TRAFs).," *Oncogene*, vol. 20, no. 44, pp. 6482–91, Oct. 2001.

[75] Y. Wang, T.-B. Liu, S. Patel, L. Jiang, and C. Xue, "The casein kinase I protein Cck1 regulates multiple signaling pathways and is essential for cell integrity and fungal virulence in Cryptococcus neoformans.," *Eukaryot. Cell*, vol. 10, no. 11, pp. 1455–64, Nov. 2011.

[76] T. J. Kannanayakal, J. R. Mendell, and J. Kuret, "Casein kinase 1 alpha associated with tau-bearing lesions of inclusion body myositis," *Neurosci. Lett.*, vol. 431, no. 2, pp. 141–145, 2008.

[77] K. A. Ahmad, G. Wang, G. Unger, J. Slaton, and K. Ahmed, "Protein Kinase CK2 - A Key Suppressor of Apoptosis," *Adv. Enzym. Regul.*, vol. 48, pp. 179–187, 2008.

[78] C. J. Rogers, P. M. Clark, S. E. Tully, R. Abrol, K. C. Garcia, W. a Goddard, and L. C. Hsieh-Wilson, "Elucidating glycosaminoglycan-protein-protein

interactions using carbohydrate microarray and computational approaches.," *Proc. Natl. Acad. Sci. U. S. A.*, vol. 108, no. 24, pp. 9747–52, Jun. 2011.

[79] B. Glimelius, B. Norling, B. Westermark, and A. Wasteson, "Composition and distribution of glycosaminoglycans in cultures of human normal and malignant glial cells.," *Biochem. J.*, vol. 172, no. 3, pp. 443–56, Jun. 1978.

[80] R. O. Hynes and A. Naba, "Overview of the matrisome--an inventory of extracellular matrix constituents and functions.," *Cold Spring Harb. Perspect. Biol.*, vol. 4, no. 1, p. a004903, Jan. 2012.

[81] G. V. Rayasam, V. K. Tulasi, R. Sodhi, J. A. Davis, and A. Ray, "Glycogen synthase kinase 3: more than a namesake.," *Br. J. Pharmacol.*, vol. 156, no. 6, pp. 885–98, Mar. 2009.

[82] H. Kim, E. Kim, J. Lee, C. H. Park, and S. Kim, "C-terminal fragments of amyloid precursor protein exert neurotoxicity by inducing glycogen synthase kinase-3β expression," *FASEB J.*, 2003.

[83] T. C. Whisenant, D. T. Ho, R. W. Benz, J. S. Rogers, R. M. Kaake, E. a Gordon, L. Huang, P. Baldi, and L. Bardwell, "Computational prediction and experimental verification of new MAP kinase docking sites and substrates including Gli transcription factors.," *PLoS Comput. Biol.*, vol. 6, no. 8, Jan. 2010.

[84] K. Michelsen, H. Yuan, and B. Schwappach, "Hide and run. Arginine-based endoplasmic-reticulum-sorting motifs in the assembly of heteromultimeric membrane proteins.," *EMBO Rep.*, vol. 6, no. 8, pp. 717–22, Aug. 2005.

[85] C. Geisler, J. Dietrich, L. Bodil, J. Kastrup, J. P. H, N. Ødum, D. Mette, B. L. Nielsen, J. Peter, H. Lauritsen, and M. D. Christensen, "Leucine-based Receptor Sorting Motifs Are Dependent on the Spacing Relative to the Plasma Membrane Leucine-based Receptor Sorting Motifs Are Dependent on the Spacing Relative to the Plasma Membrane *," *J. Biol. Chem.*, vol. 273, no. 33, pp. 21316–21323, 1998.

Appendix

Cell Culture Solutions and Immunocytochemistry

- **1x PBS**

For a final volume of 500 mL, dissolve one pack of BupH Modified Dulbecco's Phosphate Buffered Saline Pack (Pierce) in deionised H2O. Final composition:

- 8 mM Sodium Phosphate
- 2 mM Potassium Phosphate
- 40 mM Sodium Chloride
- 10 mM Potassium Chloride

Sterilize by filtering through a 0.2 m filter and store at 4ºC.

- **Complete DMEM (HeLa Cells)**

For a final volume of 1 L, when preparing DMEM medium adjust to pH 7.4 and before sterilizing add:
Fetal bovine Serum (FBS) (Gibco BRL, Invitrogen) 100 mL (10% v/v)

Notes: For cell maintenance, prior to pH adjustment add 100 U/mL penicillin and 100 mg/mL streptomycin (100 mL Streptomycin/Penicilin/Amphotericin solution (Gibco BRL, Invitrogen)).

- **10% FBS Han's F12 Nutrient Mixture + L-Glutamine (CHO)**

- F12 (Gibco, Invitrogen)	10,6g
- $NaHCO_3$ (Sigma)	1,5g
- L-Glutamine (200mM stock solution)	2mL
- Streptomycin/Penicillin/Amphotericin Solution (Gibco, Invitrogen)	10mL
- 10% FBS (Gibco, Invitrogen)	100mL

Dissolve in distilled water (d) H_2O and adjust the pH to 7.3. Finally, adjust volume to 1000 mL with dH_2O.

- **4% Paraformaldehyde**

For a final volume of 100 mL, add 4 g of paraformaldehyde to 25 mL deionised H2O. Dissolve by heating the mixture at 58ºC while stirring. Add 1-2 drops of 1 M NaOH to clarify the solution and filter (0.2 m filter). Add 50 mL of 2X PBS and adjust the volume to 100 mL with deionised H2O.

Immunoprecipitation Solutions

- **DSP**

Add 0,004g of DSP to 40 µL of DMSO. Dilute in 10mL of 1x PBS.

- **Lysis Buffer**

- 1M Tris HCl, pH 7.5	40 µL
- NP-40 10%	200 µL
- 1M NaCl	600 µL
- 0,25M EDTA	8 µL
- 100mM PMSF	40 µL
- Protease Inhibitors (1:1000)	4 µL

Adjust volume to 4 mL. Keep it on ice.

SDS-PAGE and Immunoblotting Solutions

- **LGB (Lower Gel Buffer) (4x)**

To 900 mL of deionised H2O add:

- Tris 181.65 g
- SDS 4 g

Mix until the solutes have dissolved. Adjust the pH to 8.9 and adjust the volume to 1 L with deionised H2O.

- **UGB (Upper Gel Buffer) (5x)**

To 900 mL of deionised H2O add:

- Tris 75.69 g

Mix until the solute has dissolved. Adjust the pH to 6.8 and adjust the volume to 1 L with deionised H2O.

- **30% Acrylamide/0.8% Bisacrylamide**

To 70 mL of deionised H2O add:

- Acrylamide 29.2 g
- Bisacrylamide 0.8 g

Mix until the solutes have dissolved. Adjust the volume to 100 mL with deionised H2O. Filter through a 0.2 µm filter and store at 4°C.

- **10% APS (Ammonium Persulfate)**

In 10 mL of dH2O dissolve 1 g of APS.

- **10% SDS (Sodium Dodecilsulfate)**

In 10 mL of dH2O dissolve 1 g of SDS.

- **Loading Gel Buffer (4x)**

- 1 M Tris solution (pH 6.8) 2.5 ml (250 mM)
- SDS 0.8 g (8%)
- Glycerol 4 mL (40%)
- β-Mercaptoethanol 2 mL (2%)
- Bromophenol blue 1 mg (0.01 %)

Adjust the volume to 10 mL with deionised H2O. Store in the darkness at room temperature.

- **1 M Tris (pH 6.8) Solution**

To 150 mL of deonised H2O add:

- Tris base 30.3 g

Adjust the pH to 6.8 and adjust the final volume to 250 mL.

- **10x Running Buffer**

- Tris 30.3 g (250 mM)
- Glycine 144.2 g (2.5 M)
- SDS 10 g (1%)

Dissolve in dH2O, adjust the pH to 8.3 and adjust the volume to 1 L.

- **Resolving (lower) Gel Solution (60 mL)**

	6.5%	**7.5%**
- H_2O	32 mL	29.25 mL
- 30% Acryl/0.8% Bisacryl Solution	13 mL	15 mL
- LGB (4x)	15 mL	15 mL
- 10% APS	300 µL	30 µL
- TEMED	30 µL	30 µL

- **Stacking (upper) Gel Solution (20 mL)**

	3.5%
- H_2O	13.2 mL
- 30% Acryl/0.8% Bisacryl Solution	2.4 mL
- UGB (5x)	4 mL
- 10% APS	200 µL
- 10% SDS	200 µL
- TEMED	30 µL

- **1x Transfer Buffer**

  - Tris 3.03 g (25 mM)
  - Glycine 14.41 g (192 mM)

Mix until solutes dissolution. Adjust the pH to 8.3 with HCl and adjust the volume to 800 mL with dH2O. Just prior to use add 200 mL of methanol (20%).

- **10x TBS (Tris Buffered Saline)**

  - Tris 12.11 g (10 mM)
  - NaCl 87.66 g (150 mM)

  Adjust the pH to 8.0 with HCl and adjust the volume to 1 L with dH2O.

- **10x TBST (TBS + Tween)**

  - Tris 12.11 g (10 mM)
  - NaCl 87.66 g (150 mM)
  - Tween 20 5 mL (0.05 %)

  Adjust the pH to 8.0 with HCl and adjust the volume to 1 L with dH2O.

- **Membrane Stripping Solution**

  - Tris-HCl (pH 6.7) 3.76g (62.5 mM)
  - SDS 10g (2%)
  - β-marcaptoethanol 3.5 mL (100mM)

Dissolve Tris and SDS in dH_2O and adjust with HCl to pH 6.7. Add the mercaptoethanol and adjust volume to 500 mL.

- **ECL Home-made**

Solution A – ECL Luminol Solution (Stock Solution)

- 20 mM Luminol (in DMSO)*	1.25 mL (100 µM)
- 100 mM 4-iodophenol (in DMSO)*	5 mL (2mM)
- 0.1 M Tris (pH 9.35)	125 mL (50 mM)

Adjust volume to 250 mL with dH_2O.

* Protect form the light.

Solution B – Hydrogen Peroxide